

The substellar population of the young cluster lambda Orionis

D. Barrado y Navascués^{1,2}

*Laboratorio de Astrofísica Espacial y Física Fundamental, INTA, P.O. Box 50727, E-2808
Madrid, SPAIN*

barrado@laeff.esa.es

J.R. Stauffer²

IPAC, California Institute of Technology, Pasadena, CA 91125, USA

J. Bouvier³

*Laboratoire d'Astrophysique, Observatoire de Grenoble, Université Joseph Fourier, B.P. 53,
38041 Grenoble Cedex 9, France*

R. Jayawardhana

*Department of Astronomy, University of Michigan, 830 Dennison Building, Ann Arbor, MI
48109, USA*

Jean-Charles Cuillandre

CFHT, 65-1238 Mamalahoa Highway, Kamuela, HI 96743, Hawaii, USA

ABSTRACT

By collecting optical and infrared photometry and low resolution spectroscopy, we have identified a large number of low mass stars and brown dwarf candidates belonging to the young cluster (~ 5 Myr) associated with the binary star λ Orionis. The lowest mass object found is a M8.5 with an estimated mass of $0.02 M_{\odot}$ ($\sim 0.01 M_{\odot}$ for objects without spectroscopic confirmation). For those objects with spectroscopy, the measured strength of the $H\alpha$ emission line follows a distribution similar to other clusters with the same age range, with larger

¹Visiting Astronomer, Las Campanas Observatory.

²Visiting Astronomer, Keck Observatory.

³Visiting Astronomer, CFHT Observatory.

equivalent widths for cooler spectral types. Three of the brown dwarfs have H α emission equivalent widths of order 100 Å, suggestive that they may have accretion disks and thus are the substellar equivalent of Classical T Tauri stars. We have derived the Initial Mass Function for the cluster. For the substellar regime, the index of the mass spectrum is $\alpha=0.60\pm0.06$, very similar to other young associations.

Subject headings: open clusters and associations: individual (Lambda Orionis) – stars: low-mass, brown dwarfs – stars: pre-main-sequence

1. Introduction

The Lambda Ori OB-T association, located at 400 pc (Murdin & Penston 1977) is a young stellar group which has not been studied so far in great depth. It is located inside a fossil giant molecular cloud. The O8 III star λ^1 Ori, and to a lesser extent the 11 B stars near to it, excite the HII region S 264. Making use of the Infrared Astronomical Satellite (IRAS), Zhang et al. (1989) detected a dust ring with a diameter of 9 deg centered around the star λ Ori. This ring is complementary to a shell of neutral hydrogen discovered previously by Wade (1957, 1958). There are two nearby dark clouds within this ring, namely B35 and B30, separated from λ Ori by 2.2 and 2.7 deg, respectively. Based on a H α emission survey, Duerr, Imhoff & Lada (1982), identified three stellar clusters centered around B30, B35 and λ^1 Ori, respectively. Those clusters were later confirmed from a statistical point of view by Gómez & Lada (1998).

Dolan & Mathieu (1999, 2001, 2002) collected moderately deep photometry (VRI filters) in an area about 8 sq.deg. centered on the OB association, discovering a significant population of low mass stellar members, and obtained medium resolution multifiber spectroscopy for those candidates closest to the central star. Their derived distance of 450 ± 50 pc is larger than both the distance derived by Murdin & Penston (1977) and the value derived by Hipparcos (Perryman et al. 1997) for the five stars in the central area, 380 ± 30 pc. According to Dolan and Mathieu (2002), the turn-off age for the massive stars is of order 6 Myr (see also Murdin & Penston 1977 for another age determination based on the massive stars, 4 Myr), although the star formation history might be more complex (Dolan & Mathieu 2001).

In this paper, we present additional, much deeper photometry, well beyond the hydrogen burning limit at $0.072 M_{\odot}$ (Baraffe et al. 1998). For some of the new candidate members, we have also obtained low resolution spectroscopy, which allow us to add additional clues about their membership and their substellar nature. In our study, we will assume: an age

of 5 Myr, a distance 400 pc $-(m - M)_0=8.010-$ and a reddening of $E(B - V)=0.12$ (Diplas & Savage 1994). Section 2 deals with the optical search and the near infrared counterparts in the 2MASS All Sky Survey. Section 3 presents the analysis of these datasets, whereas the results are summarized in section 4.

2. The data

2.1. Optical survey

On September 29th and 30th, 1999, we conducted an optical photometric survey around the star λ Orionis, using the CFHT 12K mosaic camera and the Cousins R and I filters. This instrument covers a projected area on the sky of 42×28 arcminutes, with a scale of about 0.2 arcsec/pix. The data were collected under photometric conditions. The reduction was performed with the standard pipeline, and the extraction of the aperture photometry was carried out within the IRAF¹ environment. The astrometric calibration was tied to the USNO-A2.0 catalog (Monet et al. 1998). Our derived coordinates, on average, should be accurate to better than 1 arcsec, except for the objects closer to the edges of each detector .

Based on the results of the wide-field imaging survey of Dolan & Mathieu (2002) – specifically their Figures 6 and 8, the separation of Lambda Ori from the B30 and B35 clusters, and the FOV of the 12K mosaic, we believe that our survey should mostly include young stars from the cluster associated with Lambda Ori. Furthermore, because of the very young age and moderate distance to the cluster, we expect the very low mass cluster stars to be well separated from field stars in a color-magnitude diagram. Figure 1 illustrates the location of λ Orionis, the dark clouds and the CFHT 12K field.

We collected two different sets of exposures, with short and long exposure times. In the first case, we exposed during 10 seconds for each filter, whereas the exposure times were 600 and 900 seconds –Cousins I and R filters, respectively, for the second set. With this method, we increased the dynamical range, and our photometry overlaps with previously published data in these filters. The zero points of the photometric calibration were derived using the data from Dolan & Mathieu (1999, 2001, 2002). Each CCD was calibrated independently. The errors can be estimated as 0.06 and 0.08 magnitudes, for the shallow and deep exposures, respectively.

¹IRAF is distributed by National Optical Astronomy Observatories, which is operated by the Association of Universities for Research in Astronomy, Inc., under contract to the National Science Foundation, USA

Figure 2 displays the optical color-magnitude diagram (CMD). Dots represent the photometry of field objects (deep images), whereas solid circles correspond to our selected candidate members (deep and shallow images). We have also added other possible, brighter members from Dolan & Mathieu (1999) as crosses. The thick, solid line corresponds to an empirical ZAMS from Barrado y Navascués et al. (2001b), whereas a 5 Myr isochrone from Baraffe et al. (1998) is displayed as a dotted line. This last isochrone, together with the brighter data by Dolan & Mathieu (1999), was used as the reference –taken into account photometric errors– for the selection of candidate members. A older isochrone (e.g., 8 Myr) would not modify in a significant manner our member selection. We used a reddening of $E(R - I)_C = 0.084$. Visual inspection of the figure indicates that there is a clear separation between the field population and the cluster sequence, as we had expected. Hence, we expect contamination of our cluster membership list from field stars to be relatively small. Table 1 lists our candidate members, extracted from both the shallow and the deep datasets. Columns 4–7 list the optical photometry derived from the shallow exposures, whereas columns 8–11 contains the data from the deep images.

Our search has a magnitude limit of $I(\text{lim}) \sim 24.0$ mag. Completeness is achieved at $R(\text{complete}) \sim 22.75$ mag and $I(\text{complete}) \sim 22.75$, based on the drop (Figure 3) in the number of detected objects for each interval in the I_c and R_c filters (Wainscoat et al. 1992; Santiago et al. 1996). For cluster members, the faint limit is set by $R(\text{complete}) \sim 22.75$ at $(R - I) = 2.5$, corresponding then to $I(\text{complete, cluster}) \sim 20.2$ mag.

2.2. 2MASS infrared photometry

The limiting magnitude of the 2MASS All Sky release (Cutri et al. 2003) is about $K_s \sim 15.5$ mag. Using a Baraffe et al. (1998) 5 Myr isochrone, and the distance and reddening of the Lambda Orionis cluster, this value corresponds to cluster members having a mass similar to $0.025 M_\odot$ ($I_c \sim 19.1$ mag). Therefore, we expect that most of our optical candidate members, except the faintest, should have a counterpart in the 2MASS catalog. Our faintest candidates, with $I_c \sim 22$, would have masses of order $0.010 M_\odot$ if they are cluster members and have an age equal to 5 Myr, according to the Baraffe et al. (2003) isochrones, the so called COND models. We have matched both datasets using a 5 arcsec radius, much larger than the combined errors of the 2MASS coordinates and our own positions. Since the surface density is not very large in this field, the object identification is generally unambiguous. 2MASS photometry, together with the coordinates (more accurate than our initial values), are provided in Table 2. This table lists the I_c magnitude, the distance between the optical and the IR source and the 2MASS coordinate, and the IR photometry and uncertainties.

Column 12 describes whether the candidate fulfills different membership criteria, and the last column contains our final membership assessment (see section 3.3).

2.3. Low resolution spectroscopy

We have collected low resolution optical spectroscopy in two different campaigns. The first one took place in November 3-5, 2002, at the Keck I telescope. We made use of LRIS with the 400 l/mm grating with a one arcsec slit. Typical integration times were 300-900 seconds. The data were processed within the IRAF environment in a standard way. The wavelength calibration is better than 0.4 Å, spectral coverage is 6250–9600 Å and the resolution is $R \sim 1100$ (6.0 Å around $H\alpha$), as measured in a NeAr lamp. For the second run, we used the B&C spectrograph attached to the Magellan II telescope in March 9-11, 2003. The reduction was carried out in a similar way as in the case of the Keck sample. The Magellan spectra have slightly worse resolution and larger spectral range ($R \sim 800$, 5000-10200 Å), since in this case we used the 300 l/mm grating. Relative flux calibration for the spectra was derived using observations obtained of several spectrophotometric standards.

In total, we obtained spectra for 33 objects out of the 170 possible members discovered in our optical survey. The spectra are displayed in Figure 4a-d. Panels a, b and c correspond to data from Keck I, whereas panel d contains the Magellan spectra.

3. Analysis

3.1. Spectral types

Simultaneously to our observations of Lambda Orionis candidate members, we observed a large number of cool stars of different luminosity classes (V, IV and III) and spectral types ranging from K7 to M9. These spectra were reduced in the same way and were used to measure spectral indices as defined by Martín et al. (1996, 1999) and Kirkpatrick et al. (1999). Then, we calibrated these indices with the known spectral types of this dataset, and derived spectral types for our candidate members. A final visual inspection was carried out, by comparing the spectrum of the cluster candidate member with the one corresponding to a field star of the same spectral type. The final values are listed in Table 3. The error in the spectral type assignation, except in one case (LOri-CFHT-165), can be estimated as half a subclass.

3.2. Color - color, color-magnitude and magnitude versus spectral type diagrams

Figures 5a and 5b display optical-infrared color-magnitudes diagrams, whereas color-color diagrams are illustrated in Figures 6a, 6b and 6c. In these diagrams, we have over-plotted 5 Myr isochrones by Baraffe et al. (1998, 2002) and Chabrier et al. (2000), shifting them to a distance of 400 pc, and using the interstellar extinctions of $A_R=0.307$, $A_I=0.223$, $A_J=0.106$, $A_H=0.066$, and $A_K=0.04$. Additionally, the Ic and Ks magnitudes versus the spectral type are shown in Figures 7a and 7b. In these last two cases, we made use of temperature scales by Luhman (1999) -dotted lines– and Basri et al. (2000) -solid line–for the conversion between effective temperatures and spectral types. Note that Luhman’ scales were derived for giant and dwarfs, and for an intermediate gravity, which roughly describes the location of Lambda Ori cluster members, whose gravity should be $\log g \simeq 4.0$, according to Baraffe et al. (1998) models. In all these figures, different symbols represent our membership assignments (see next subsection).

3.3. Membership

We have established a membership status based on two main criteria: the spectroscopic and photometric information. When the first one was available, we relied mainly on it, otherwise we made use of the optical-infrared photometry.

1.- Candidates with spectroscopy.

1.a.- Both spectral type and photometric data in agreement with cluster sequence. Probable members. They appear with the label “Mem+” in Table 2, and displayed in Figures 5-9 as solid circles.

1.b.- Spectral type compatible with cluster sequence, but the location in one or two CCD or CMD does not correspond to a member. Possible members. Label “Mem?” (solid triangles).

1.c.- The estimated spectral type does not agree with the photometry, but all CMD and CCD indicate membership. We also have included here L Ori-CFHT-119, with photometry in disagreement with membership and whose spectral type does not indicate clearly its status. Possible non-member. “NM?” (open triangles).

1.d. -Both spectral type and photometric data in disagreement with cluster sequence. Probable non-members. “NM+” (open circles).

2.- Candidates without spectroscopy.

2.a.- All CMD and CCD indicate membership. Probable members. They are listed in Table 2 with the tag “Mem”. Shown as plus symbols in Figures 5-9.

2.b.- One CMD or CCD in disagreement with the cluster sequence. Possible members. “Mem?” (crosses).

2.c.- At least a CMD and another CMD or CCD in disagreement with the membership. Possible non-member. “NM-” (small dots).

2d.- No information in the 2MASS All Sky release. Most of them are too faint to have been detected by that survey. They are labeled with the tag “???”.

One object, LOri-081, is located in Figure 5b in a position which might indicate a large reddening. However, Figures 6a and 6b suggest that this object has a near infrared excess which is characteristic of Classical TTauri stars. Note, however, that its $H\alpha$ equivalent width is not very large (see section 3.5). Since this low mass star has no other indicator which might suggest it is a non-member, we have catalogued it as a member.

Figure 8a shows the absolute I_c magnitude against the dereddened $(R - I)_c$ color and a comparison with theoretical isochrones with ages in the range 1-10 Myr by Baraffe et al. (1998) –NextGen models. Figure 8b displays the same set of theoretical models (isochrones and evolutionary tracks) in a HR diagram. Luminosities were derived from either the I_c or the K_s magnitudes –open squares or stars, respectively– and bolometric corrections by Comerón et al. (2000) and Tinney et al. (1993). Effective temperatures come from the Luhman’s scale (1999) for intermediate gravity. This figure indicates that the age of the cluster is bracketed by 3 and 10 Myr.

Of the 170 candidate members selected from the $(R, R-I)$ CMD, 24 have no IR data, and of the remaining 146, 104 are classified probable members, 22 as possible members and 20 as non members. Hence, the contamination level of the optical sample is of order of 25% for both subsamples with and without spectral information. Additionally, a significant fraction of the confirmed members should be, based on the assumed distance, reddening and age ranges, bona fide brown dwarfs.

3.4. Spatial distribution

We have checked whether there is any concentration of bona fide, probable or possible members close to the λ Orionis multiple star (or, conversely, a clustering of non-members).

Figure 9 shows the spatial distribution. We see no conclusive evidence for clustering or sub-clustering. Due to the geometry of our survey (a rectangle of 42×28 arcmin) and the total area covered by it (smaller than the expected projected total size of the cluster about 1-2 sq.deg), we have not derive the radial distribution of objects.

3.5. The Mass Function

We have derived the cluster’s Initial Mass Function (IMF) in the mass range 0.02 - $1.2 M_{\odot}$ (the CFHT 1999 RI survey) and from Dolan & Mathieu’s (1999, 2001) brighter sample over the mass range 0.3 - $4.7 M_{\odot}$. We used two sets of data: In the first one we removed the probable non-members (NM+). In the second set, we only retained the probable members (“Mem+” and “Mem”). Masses were computed from dereddened I-band magnitudes, using 3, 5 and 10 Myr isochrones of Baraffe et al.’s (1998) model. Note that, as shown in Barrado y Navascués et al. (2001b), the use of other models do not affect the derived IMF in an significant degree.

The cluster’s MF is shown in Figure 10a, where Dolan & Mathieu’s sample has been restricted to the area in common with the CFHT 1999 survey. The vertical segment denotes the location of the completeness limit of the CFHT survey. A power law fit –carried out with the sample without the probable non-members– to the mass spectrum ($dN/dm \propto m^{-\alpha}$) indicates an index $\alpha = +0.60 \pm 0.06$ across the stellar/substellar limit (0.03 - $0.14 M_{\odot}$), and a slightly steeper index $\alpha = +0.86 \pm 0.05$ over the whole mass range from $\sim 0.024 M_{\odot}$ to $0.86 M_{\odot}$, using a 5 Myr isochrone. A 5 Myr isochrone from Burrows et al. (1997) gives $\alpha = +0.69 \pm 0.17$ in the range 0.20 - $0.015 M_{\odot}$, whereas models from D’Antona & Mazzitelli (1997, 1998) are almost identical –regarding the power law index– to those obtained with Baraffe et al. (1998).

On the other hand, 3 and 10 Myr isochrones from Baraffe et al. (1998) yield $\alpha = +0.92 \pm 0.04$ and $\alpha = +0.71 \pm 0.06$, respectively (again, in the range $0.024 M_{\odot}$ to $0.86 M_{\odot}$).

In the case of second dataset, which only contains bona-fide members, the slope of the IMF, for a 5 Myr isochrone, is $\alpha = +0.57 \pm 0.06$. Note, however, that this is a minimum value, since some among the faintest candidate members do not have IR data (they do not appear in the 2MASS catalog) and because our spectroscopic survey was biased (we observed preferably in the range $I_c=15$ -17).

The slope of Lambda Ori MF at lower masses and into the substellar domain is quite similar to that derived for other young clusters by some of us, e.g. Sigma Orionis ($\alpha = +0.8$, Béjar et al. 2001), Alpha Per ($\alpha = +0.6$, Barrado y Navascués et al. 2002b) and the Pleiades ($\alpha = +0.6$, Bouvier et al. 1998; Moraux et al. 2003). The age of these clusters is estimated

as 5, 80 and 125 Myr, respectively (Zapatero Osorio et al. 2002; Stauffer et al. 1998, 1999; Barrado y Navascués et al. 2004). The α index is also similar to the results obtained in other stellar associations such as Trapezium, IC348 or Taurus (Luhman et al. 2000, 2003; Lucas & Roche 2000; Hillenbrand & Carpenter 2000; Najita et al. 2000; Preibisch et al. 2002; Briceño et al. 2002; Muench et al. 2003).

Figure 10b displays the same data but plotted as $dN/d\log M$ (instead of dN/dM) as a function of mass. The cluster’s mass function appears to rise from 3 to $0.8 M_{\odot}$, remains about flat down to $0.1 M_{\odot}$, and decreases toward lower masses and into the substellar regime. This behaviour is not unlike the lognormal shape of the mass function derived for both the Pleiades cluster (Moraux et al. 2003), as illustrated on Fig. 10b with a dashed line, and the galactic field (Chabrier 2003).

3.6. $H\alpha$ emission

We have measured the $H\alpha$ equivalent with using the pseudo-continuum. Note that low resolution spectra tend to produce larger equivalent widths compared with data taken at higher resolution. These values, plotted versus the derived spectral types with symbols as in the previous figures, are displayed in Figure 11, where we also include a comparison with the “twin” cluster sigma Orionis (Wolk 1996; Walter et al. 1997), with approximately the same age and located at similar distance. Sigma Orionis $H\alpha$ equivalent widths and spectral types come from Béjar et al. (1999), Barrado y Navascués et al. (2001a, 2002a, 2003), Zapatero Osorio et al. (2002), Muzerolle et al. (2003), and Jayawardhana, Mohanty & Basri (2003). The dashed lines indicate the 5 and 20 Å criteria which separate Classical -accreting- from Weak-line -non accreting- T Tauri stars, whereas the thick line corresponds to the criterion differentiating accreting from non accreting objects, based on low resolution spectroscopy (Barrado y Navascués & Martín 2003). This criterion is based on the upper envelope of chromospheric $H\alpha$ emission present in cluster members belonging IC2391, Alpha Per and the Pleiades. Although the low resolution and relatively low S/N of our spectra –especially at the faint end– do not allow us to definitively prove that any of our objects have accretion disks (Muzerolle et al. 2003; Jayawardhana, Mohanty & Basri 2003), the strength of $H\alpha$ for several of the confirmed members of the Lambda Ori cluster suggests to us that some of them might be accreting.

The three Lambda Ori members with strongest $H\alpha$ emission are: L Ori 140 (eq. width = 72.8 Å), L Ori 156 (eq. width = 101.7 Å) and L Ori 161 (eq. width = 123 Å). L Ori 140 might present [OI]6300 in emission. Note that all of the objects with the largest $H\alpha$ equivalent widths are located in the substellar regime of the CMD. However, we do not detect [OII]7329

Å, [SII]6717&6731 Å or the CaII IRT, which can be seen in LS-RCrA 1, another brown dwarf of similar mass and spectral type (M6.5 IV), discovered by Fernández & Comerón (2001) and analyzed in depth by Barrado y Navascués, Mohanty & Jayawardhana (2004). The spectral properties of these three members are closer to those present in 2M1207-3932, a M8 brown dwarf which belong to the TW Hydrae association (Mohanty et al. 2003).

4. Summary and Conclusions.

We have collected deep optical photometry in about 0.3 sq.deg around the binary star λ Orionis, extending to well below the substellar boundary. The combination of this dataset set with near infrared photometry and low resolution spectroscopy –i.e., spectral types– allow us to cull from the initial membership list the possible and probable low mass members of the cluster, both of stellar and substellar nature. We note, however, that additional work is required, in order to study other youth indicators such as low-gravity features and the detection of lithium. We conclude that the pollution fraction due to interlopers is low (similar to 25 % for both the sample with or without spectroscopic information). The faintest object whose membership has been established is a brown dwarf with a mass slightly below $0.020 M_{\odot}$ (based on the Chabrier and Baraffe models) and a M8.5 spectral type. Moreover, $H\alpha$ equivalent widths have been measured in the spectra. A plot of the $H\alpha$ equivalent widths as a function of spectral type shows a very similar distribution for Lambda Ori and for the similar age Sigma Ori clusters, with an increase on average for cooler spectral types. Some of the Lambda Orionis stars and brown dwarfs have $W(H\alpha)$ larger than the chromospheric saturation limit. By analogy with Classical TTauri stars, they might have an accretion disk. We have also derived the Initial Mass Function in the range 4.7-0.02 M_{\odot} , which shows different types of behavior when displayed as a mass spectrum. Across the stellar/substellar boundary, the index of a power law fit is $\alpha=+0.60\pm 0.06$, quite similar to values recently derived for other young clusters in the same mass range.

We do appreciate the referee’s comments and suggestions (Victor Béjar). DByN is supported by the Spanish “Programa Ramón y Cajal”, PNAyA2001-1124-C02 and PNAyA AYA2003-05355. This publication makes use of data products from the Two Micron All Sky Survey.

REFERENCES

Baraffe I., Chabrier G., Allard F., Hauschildt P. H., 1998, A&A, 337, 403

- Baraffe I., Chabrier G., Allard F., Hauschildt P. H., 2002, A&A, 382, 563
- Baraffe I., Chabrier G., Barman T.S., Allard F., Hauschildt P.H., 2003, A&A 402, 701
- Barrado y Navascués D., Zapatero Osorio M.R., Béjar V.J.S. et al. 2001a, A&A Letters 377, 9
- Barrado y Navascués D., Stauffer J.R., Bouvier J., Martín E.L., 2001b, ApJ 546, 1006
- Barrado y Navascués D., Zapatero Osorio M.R., Martín E.L., Béjar V.J.S., Rebolo R., Mundt R., 2002a, A&A Letters 393, 85
- Barrado y Navascués D., Bouvier J., Stauffer J.R., Lodieu N., McCaughrean M.J., 2002b, A&A 395, 813
- Barrado y Navascués D., Béjar V.J.S., Mundt R., Martín R., Rebolo R., Zapatero Osorio M.R., Bailer-Jones C.A.L., 2003, A&A 404, 171
- Barrado y Navascués D., Martín E.L., 2003, AJ 126, 2997
- Barrado y Navascués D., Mohanty S., Jayawardhana R., 2004, ApJ 604, 284
- Barrado y Navascués D., Stauffer J.R., Jayawardhana R., 2004, ApJ, in prep.
- Basri G., Mohanty S., Allard F., et al., 2000, ApJ, 538, 363
- Béjar V.J.S., Zapatero Osorio M.R., Rebolo R., 1999, ApJ 521, 671
- Béjar V. J. S., Martín E. L., Zapatero Osorio M. R., et al., 2001, ApJ, 556, 830
- Bessell M.S., Brett J.M., 1988, PASP 100, 1134
- Bouvier J., Stauffer J.R., Martín, E.L., Barrado y Navascués, D., Wallace B., Béjar, V., 1998, A&A 336, 490
- Briceño, C., Luhman, K. L., Hartmann, L., Stauffer, J. R., & Kirkpatrick, J. D. 2002, ApJ 580, 317
- Chabrier G., Baraffe I., , Allard F., Hauschildt P., 2000, ApJ, 542, L119.
- Chabrier G., 2003, PASP 115, 763
- Comerón F., Neuheuser R., Kaas A.A., 2000 A&A 359, 269

- Cutri R.M., et al. 2003, “2MASS All-Sky Catalog of Point Sources”, University of Massachusetts and Infrared Processing and Analysis Center, (IPAC/California Institute of Technology).
- Diplas A., Savage B.D. 1994, *ApJS*, 93, 211
- Duerr R., Imhoff C.L., Lada C.J., 1982, *ApJ* 261, 135
- Dolan C.J & Mathieu R.D., 1999, *AJ* 118, 2409
- Dolan C.J & Mathieu R.D., 2001, *AJ* 121, 2124
- Dolan C.J & Mathieu R.D., 2002, *AJ* 123, 387
- Gómez M., & Lada C.J., 1998, *AJ* 115, 1524
- Hillenbrand L.A., Carpenter J.M., 2000, *ApJ* 540, 236
- Jayawardhana R., Mohanty S., Basri G., 2003, *ApJ* 592, 282
- Kirkpatrick D., Reid I. N., Liebert J., et al., 1999, *ApJ*, 519, 802
- Kirkpatrick J.D. et al. 2000, *AJ* 120, 447
- Leggett S.K., Allard F., Geballe T.R., Hauschildt P.H., Schweitzer A., 2001, *ApJ* 548 908
- Lucas P.W., Roche P.F., 2000, *MNRAS* 314, 858
- Luhman K.L. 1999, *ApJ*, 525, 466
- Luhman K.L., 2000, *ApJ* 544, 1044
- Luhman, K.L., Briceño, C., Stauffer, J.R., Hartmann, L., Barrado y Navascués, D., Caldwell, N., 2003, *ApJ*, 590, 348
- Martín E. L., Rebolo R., Zapatero Osorio M.R., 1996, *ApJ* 496, 706
- Martín E. L., Delfosse X., Basri G., et al. 1999, *AJ*, 118, 2466
- Meyer M.R., Calvet N., Hillenbrand L.A., 1997, *AJ* 114, 288
- Mohanty S., Jayawardhana R., Barrado y Navascués D., 2003, *ApJ Letters* 593, 109
- Monet D., Bird A., Canzian B., et al. 1998, U.S. Naval Observatory Flagstaff Station (USNOFS) and Universities Space Research Association (USRA) stationed at USNOFS.

- Moraux E., Bouvier J., Stauffer J.R., Cuillandre J.-C., 2003, *A&A* 400, 891
- Muench A.A., Lada E.A., Lada C.J., Elston R.J., Alves J.F., Horrobin M., Huard T.H., Levine J.L., Raines S.N., Román-Zúñiga C. 2003, *AJ* 125, 2029
- Murdin P., & Penston M.V., 1997, *MNRAS* 181, 657
- Muzerolle J., Hillenbrand L., Calvet N., Briceñ C., Hartmann L., 2003, *ApJ* 592, 266
- Najita J., Tiede G.P., Carr J.S., 2000, *ApJ* 541, 977
- Perryman M.A.C., Lindegren L., Kovalevsky J., et al. 1997, *A&A Letters*.323, 49
- Preibisch T., Brown A.G.A., Bridges T., Guenther E., Zinnecker H., 2002, *AJ* 124, 404
- Santiago B.X., Gilmore G., Elson R.A.W., 1996, *MNRAS* 281, 871
- Stauffer J.R., Schultz G., Kirkpatrick J.D., 1998, *ApJ Letters* 499, 199
- Stauffer J.R., Barrado y Navascués D., Bouvier J., et al. 1999, *ApJ* 527, 219
- Tinney C.G., Mould J.R., Reid I.N., 1993, *AJ* 105, 1045
- Wade C.M., 1957, *AJ* 62, 148
- Wade C.M., 1958, Ph.D. thesis, Harvard University
- Wainscoat R.J., Cohen M., Volk K., Walker H.J., Schwartz D.E., 1992, *ApJ Suppl.*, 83, 111
- Walter F.M., Wolk S.J., Freyberg M., Schmitt J.H.M.M., 1997, *Mem.Soc.Astron.It.* 68, 1081
- Wolk S.J., 1996, Ph.D. thesis, Univ. New York at Stony Brook
- Zhang C.Y., Laureijs R.J., Chlewicki G., Clark F.O., Wesselius P.R., 1989, *A&A* 218, 231
- Zapatero Osorio M.R., Béjar V.J.S., Pavlenko Ya., Rebolo R., Allende Prieto C., Martín E.L., García López R.J., 2002a, *A&A* 384, 937.

Table 1: Positions and optical photometric data for our lambda Orionis candidate members.

L Ori	R.A	DEC	Ic	(R-I)c	δR	δI	Ic	(R-I)c	δR	δI
CFHT	(2000.0)		shallow exp.				deep exp.			
#	(h:m:s)	($^{\circ}$ ' ")								
001	5:33:47.18	9:55:38.5	12.52	0.69	0.01	0.01	—	—	—	—
002	5:36:10.36	10:08:54.9	12.64	0.80	0.01	0.01	—	—	—	—
003	5:35:55.44	9:56:31.5	12.65	0.74	0.01	0.01	—	—	—	—
004	5:35:47.55	9:45:50.5	12.65	1.06	0.01	0.01	—	—	—	—
005	5:33:53.65	9:43:07.97	12.67	0.71	0.01	0.01	—	—	—	—
006	5:35:16.26	9:55:17.8	12.75	0.80	0.01	0.01	—	—	—	—
007	5:34:29.55	9:48:58.7	12.78	0.94	0.01	0.01	—	—	—	—
008	5:35:57.97	9:54:32.8	12.79	0.81	0.01	0.01	—	—	—	—
009	5:34:46.34	10:06:35.6	12.95	0.75	0.01	0.01	—	—	—	—
010	5:34:32.96	10:08:41.1	12.96	0.74	0.01	0.01	—	—	—	—
011	5:34:44.66	9:53:57.5	13.01	0.83	0.01	0.01	—	—	—	—
012	5:35:05.95	9:52:07.8	13.03	0.77	0.01	0.01	—	—	—	—
013	5:33:56.35	9:53:56.69	13.03	1.18	0.01	0.01	—	—	—	—
014	5:36:19.03	10:03:50.8	13.03	0.81	0.01	0.01	—	—	—	—
015	5:34:21.84	10:04:14.5	13.05	0.78	0.01	0.01	—	—	—	—
016	5:35:13.50	9:55:24.5	13.18	0.89	0.01	0.01	—	—	—	—
017	5:36:20.49	9:52:19.3	13.19	0.80	0.01	0.01	—	—	—	—
018	5:36:16.59	9:50:48.8	13.26	0.95	0.01	0.01	—	—	—	—
019	5:35:13.69	9:56:28.8	13.31	1.02	0.01	0.01	—	—	—	—
020	5:34:57.57	9:46:07.5	13.31	1.34	0.01	0.01	—	—	—	—
021	5:35:06.94	9:48:57.8	13.38	0.88	0.01	0.01	—	—	—	—
022	5:35:51.35	9:55:10.8	13.38	1.03	0.01	0.01	—	—	—	—
023	5:35:57.65	9:47:34.6	13.44	0.99	0.01	0.01	—	—	—	—
024	5:34:57.11	9:54:36.1	13.45	0.98	0.01	0.01	—	—	—	—
025	5:36:20.18	9:44:02.0	13.45	0.91	0.01	0.01	—	—	—	—
026	5:34:36.20	9:53:43.8	13.47	1.10	0.01	0.01	—	—	—	—
027	5:35:11.01	10:07:36.7	13.50	0.99	0.01	0.01	—	—	—	—
028	5:36:18.85	9:51:35.3	13.65	1.21	0.01	0.01	—	—	—	—
029	5:35:25.36	10:08:38.7	13.69	1.20	0.01	0.01	—	—	—	—
030	5:35:12.57	9:55:18.8	13.74	1.21	0.01	0.01	—	—	—	—
031	5:34:49.02	9:58:03.4	13.75	1.15	0.01	0.01	—	—	—	—
032	5:36:09.31	9:47:03.7	13.80	1.24	0.01	0.01	—	—	—	—
033	5:35:34.83	10:00:35.1	13.81	1.01	0.01	0.01	—	—	—	—
034	5:35:19.92	10:02:36.6	13.97	1.13	0.01	0.01	—	—	—	—
035	5:35:15.16	10:01:07.1	13.97	1.28	0.01	0.01	—	—	—	—
036	5:34:39.25	10:01:29.4	13.98	1.49	0.01	0.01	—	—	—	—
037	5:34:35.57	9:59:44.3	13.99	1.18	0.01	0.01	—	—	—	—
038	5:33:49.96	9:50:37.3	14.01	1.09	0.01	0.01	—	—	—	—
039	5:35:57.06	9:46:53.0	14.02	1.23	0.01	0.01	—	—	—	—
040	5:35:39.49	9:50:33.0	14.06	1.32	0.01	0.01	—	—	—	—
041	5:35:30.47	9:50:34.5	14.10	1.45	0.01	0.01	—	—	—	—
042	5:36:07.12	10:09:48.0	14.14	1.17	0.01	0.01	—	—	—	—
043	5:35:02.73	9:56:49.4	14.16	1.30	0.01	0.01	—	—	—	—
044	5:34:08.38	9:51:25.27	14.17	1.22	0.01	0.01	—	—	—	—
045	5:35:07.40	9:58:23.8	14.23	1.33	0.01	0.01	—	—	—	—
046	5:34:26.08	9:51:49.7	14.36	1.28	0.01	0.01	—	—	—	—
047	5:35:55.64	9:50:53.7	14.38	1.53	0.01	0.01	—	—	—	—
048	5:35:12.58	9:53:10.8	14.41	1.37	0.01	0.01	—	—	—	—
049	5:35:01.00	9:49:36.4	14.50	1.27	0.01	0.01	—	—	—	—
050	5:34:56.39	9:55:03.8	14.54	1.36	0.01	0.01	—	—	—	—

Table 1: Positions and optical photometric data for our lambda Orionis candidate members.

L Ori CFHT #	R.A. (2000.0) (h:m:s)	DEC (2000.0) (° ' ")	Ic	(R-I)c shallow exp.	δR	δI	Ic	(R-I)c deep exp.	δR	δI
051	5:36:12.14	10:00:57.4	14.60	1.31	0.01	0.01	—	—	—	—
052	5:34:11.77	9:57:03.91	14.63	1.30	0.01	0.01	—	—	—	—
053	5:34:36.71	9:52:58.1	14.72	1.36	0.01	0.01	—	—	—	—
054	5:35:52.52	9:48:31.6	14.73	1.46	0.01	0.01	—	—	—	—
055	5:35:21.43	9:49:56.9	14.76	1.36	0.01	0.01	—	—	—	—
056	5:34:58.36	9:53:46.7	14.87	1.56	0.01	0.01	—	—	—	—
057	5:35:11.35	10:00:50.8	15.04	1.59	0.01	0.01	—	—	—	—
058	5:36:10.37	10:00:19.1	15.06	1.51	0.01	0.01	—	—	—	—
059	5:34:23.57	9:43:43.3	15.10	1.47	0.01	0.01	—	—	—	—
060	5:35:20.00	9:49:06.6	15.14	1.42	0.01	0.01	—	—	—	—
061	5:35:18.19	9:52:24.2	15.15	1.43	0.01	0.01	—	—	—	—
062	5:35:15.33	9:48:37.3	15.16	1.46	0.01	0.01	—	—	—	—
063	5:35:19.16	9:54:41.9	15.34	1.46	0.01	0.01	—	—	—	—
064	5:35:51.99	9:50:29.8	15.34	1.44	0.01	0.01	—	—	—	—
065	5:35:17.95	9:56:58.4	15.37	1.52	0.01	0.01	—	—	—	—
066	5:35:06.76	9:57:29.5	15.40	1.72	0.01	0.01	—	—	—	—
067	5:36:26.37	9:45:46.8	15.53	1.52	0.01	0.01	—	—	—	—
068	5:34:48.01	9:43:25.82	15.20	1.56	0.01	0.01	—	—	—	—
069	5:34:43.96	9:48:35.71	15.20	1.69	0.01	0.01	—	—	—	—
070	5:36:00.03	10:05:49.0	15.61	1.57	0.01	0.01	—	—	—	—
071	5:34:15.78	10:06:54.44	15.45	1.64	0.01	0.01	15.63	1.50	0.01	0.01
072	5:34:11.34	9:42:06.35	15.35	1.65	0.01	0.01	—	—	—	—
073	5:34:46.82	9:50:37.88	15.28	1.56	0.01	0.01	—	—	—	—
074	5:36:00.57	9:42:38.15	15.39	1.64	0.01	0.01	—	—	—	—
075	5:34:55.22	10:00:35.31	15.23	1.72	0.01	0.01	—	—	—	—
076	5:35:11.00	9:57:45.0	15.81	1.58	0.01	0.01	—	—	—	—
077	5:34:41.68	9:42:41.13	15.82	1.61	0.01	0.01	15.89	1.56	0.01	0.01
078	5:36:16.43	9:50:16.42	15.79	1.54	0.01	0.01	15.92	1.43	0.01	0.01
079	5:34:48.27	9:59:54.63	15.89	1.60	0.01	0.01	16.00	1.51	0.01	0.01
080	5:35:30.04	9:59:25.84	15.65	1.75	0.01	0.01	16.01	1.50	0.01	0.01
081	5:33:56.64	10:06:14.70	15.98	1.63	0.01	0.01	16.02	1.59	0.01	0.01
082	5:36:00.80	9:52:57.40	15.92	1.63	0.01	0.01	16.02	1.55	0.01	0.01
083	5:35:43.44	9:54:26.28	15.94	1.60	0.01	0.01	16.02	1.54	0.01	0.01
084	5:35:50.83	10:09:46.32	15.78	1.62	0.01	0.01	16.03	1.45	0.01	0.01
085	5:35:21.54	9:53:29.0	16.04	1.61	0.01	0.01	—	—	—	—
086	5:34:11.56	9:49:15.61	—	—	—	—	16.09	1.50	0.01	0.01
087	5:34:33.72	9:55:33.44	16.16	1.59	0.01	0.01	16.09	1.45	0.01	0.01
088	5:34:49.51	9:58:47.86	16.04	1.72	0.01	0.01	16.10	1.68	0.01	0.01
089	5:35:04.00	10:07:26.66	16.13	1.66	0.01	0.01	16.15	1.64	0.01	0.01
090	5:36:27.06	9:51:35.09	16.15	1.62	0.01	0.01	16.17	1.60	0.01	0.01
091	5:34:35.82	9:54:25.99	16.16	1.83	0.01	0.01	16.18	1.83	0.01	0.01
092	5:35:50.95	9:51:03.86	16.18	1.64	0.01	0.01	16.19	1.65	0.01	0.01
093	5:34:41.19	9:50:16.34	16.18	1.63	0.01	0.01	16.21	1.61	0.01	0.01
094	5:34:43.18	10:01:59.92	16.29	1.76	0.02	0.01	16.28	1.75	0.01	0.01
095	5:35:24.21	9:55:14.94	16.31	1.64	0.01	0.01	16.35	1.61	0.01	0.01
096	5:35:11.17	9:57:20.9	16.37	1.65	0.02	0.01	—	—	—	—
097	5:35:09.26	9:45:59.5	16.39	1.62	0.01	0.01	—	—	—	—
098	5:36:31.53	9:45:01.41	16.41	1.72	0.02	0.01	16.40	1.72	0.01	0.01
099	5:34:45.59	10:05:48.64	16.45	1.68	0.02	0.01	16.42	1.72	0.01	0.01
100	5:35:00.11	9:46:14.34	16.45	1.63	0.01	0.01	16.43	1.65	0.01	0.01

Table 1: Positions and optical photometric data for our lambda Orionis candidate members.

LOri CFHT #	R.A (2000.0) (h:m:s)	DEC ($^{\circ}$ ' ")	Ic	(R-I)c shallow exp.	δR	δI	Ic	(R-I)c deep exp.	δR	δI
101	5:36:30.50	10:08:55.52	16.57	1.60	0.01	0.01	16.48	1.66	0.01	0.01
102	5:35:22.04	9:52:52.19	16.51	1.75	0.02	0.01	16.50	1.74	0.01	0.01
103	5:35:22.56	9:45:02.12	16.58	1.72	0.02	0.01	16.55	1.75	0.01	0.01
104	5:35:07.05	9:54:01.1	16.71	1.77	0.03	0.01	—	—	—	—
105	5:34:17.57	9:52:30.14	16.78	1.78	0.02	0.01	16.75	1.83	0.01	0.01
106	5:35:28.80	9:54:09.92	16.79	1.71	0.02	0.01	16.76	1.72	0.01	0.01
107	5:35:55.17	9:52:20.35	16.85	1.99	0.04	0.01	16.78	2.07	0.01	0.01
108	5:35:26.03	10:08:10.05	16.75	1.88	0.03	0.01	16.80	1.84	0.01	0.01
109	5:34:08.54	9:50:43.57	16.87	1.78	0.01	0.01	16.81	1.86	0.01	0.01
110	5:35:32.63	9:52:48.87	16.83	1.65	0.02	0.01	16.82	1.72	0.01	0.01
111	5:34:19.55	10:09:08.83	16.91	1.92	0.03	0.01	16.86	2.02	0.01	0.01
112	5:34:33.57	9:43:55.59	16.94	1.79	0.03	0.01	16.87	1.85	0.01	0.01
113	5:33:47.92	10:01:39.62	17.01	1.70	0.03	0.01	16.99	1.72	0.01	0.01
114	5:36:18.10	9:52:25.53	17.08	1.92	0.04	0.01	17.06	1.93	0.01	0.01
115	5:34:46.32	10:02:32.00	—	—	—	—	17.08	1.72	0.01	0.01
116	5:35:12.07	10:01:04.75	17.25	1.84	0.04	0.01	17.17	1.88	0.01	0.01
117	5:35:07.95	10:00:06.25	17.26	1.93	0.06	0.01	17.21	2.03	0.01	0.01
118	5:35:24.42	9:53:51.73	17.25	1.84	0.04	0.01	17.23	1.87	0.01	0.01
119	5:34:19.49	9:42:22.73	17.35	1.76	0.04	0.01	17.30	1.81	0.01	0.01
120	5:34:46.20	9:55:36.90	17.36	1.83	0.04	0.01	17.34	1.89	0.01	0.01
121	5:34:34.37	9:42:16.61	—	—	—	—	17.37	1.75	0.01	0.01
122	5:34:35.43	9:51:18.71	17.45	1.84	0.05	0.01	17.38	1.93	0.01	0.01
123	5:34:20.47	10:05:22.4	17.42	2.11	0.06	0.01	—	—	—	—
124	5:34:14.24	9:48:26.97	—	—	—	—	17.45	1.85	0.01	0.01
125	5:34:14.24	9:48:26.9	17.51	1.78	0.04	0.01	—	—	—	—
126	5:35:39.88	9:53:23.64	17.56	1.94	0.06	0.01	17.52	2.00	0.01	0.01
127	5:34:11.26	9:51:30.70	17.53	2.34	0.10	0.01	—	—	—	—
128	5:35:06.29	9:58:02.82	17.62	1.95	0.07	0.01	17.58	1.95	0.01	0.01
129	5:36:09.84	9:42:37.44	17.60	1.86	0.05	0.01	17.59	1.92	0.01	0.01
130	5:34:56.54	9:42:32.45	17.64	1.81	0.05	0.01	17.63	1.81	0.01	0.01
131	5:36:07.02	9:52:51.65	17.61	2.08	0.07	0.01	17.78	2.01	0.01	0.01
132	5:34:29.18	9:47:07.70	17.86	2.14	0.09	0.01	17.82	2.17	0.01	0.01
133	5:36:13.95	10:08:10.69	—	—	—	—	17.83	1.85	0.01	0.01
134	5:35:22.88	9:55:06.65	17.92	2.17	0.11	0.01	17.90	2.01	0.01	0.01
135	5:35:09.35	9:52:43.94	17.93	1.88	0.08	0.01	17.90	2.01	0.01	0.01
136	5:34:38.31	9:58:13.1	17.92	2.14	0.12	0.01	—	—	—	—
137	5:36:30.91	10:05:13.5	17.96	1.93	0.08	0.09	—	—	—	—
138	5:33:43.44	9:45:22.81	18.03	2.07	0.11	0.01	17.96	2.05	0.01	0.01
139	5:35:44.34	10:05:54.11	—	—	—	—	18.16	1.88	0.01	0.01
140	5:34:19.29	9:48:28.02	18.25	2.08	0.12	0.02	18.21	2.13	0.01	0.01
141	5:35:38.08	9:51:05.22	18.83	2.07	0.22	0.03	18.25	2.19	0.01	0.01
142	5:34:17.00	10:06:16.42	18.36	2.06	0.14	0.02	18.27	2.07	0.01	0.01
143	5:35:00.94	9:58:21.59	—	—	—	—	18.30	2.02	0.01	0.01
144	5:34:20.07	9:59:27.3	18.30	1.94	0.11	0.11	—	—	—	—
145	5:36:32.83	9:56:01.10	—	—	—	—	18.37	2.28	0.02	0.01
146	5:35:00.15	9:52:40.7	18.60	2.28	0.26	0.02	—	—	—	—
147	5:35:06.30	9:46:54.24	—	—	—	—	18.60	1.94	0.01	0.01
148	5:36:29.00	9:43:21.45	18.58	2.17	0.20	0.03	18.62	2.15	0.02	0.01
149	5:33:42.75	10:05:33.02	—	—	—	—	18.95	2.12	0.02	0.01
150	5:35:07.48	9:49:33.64	—	—	—	—	19.00	2.29	0.03	0.01

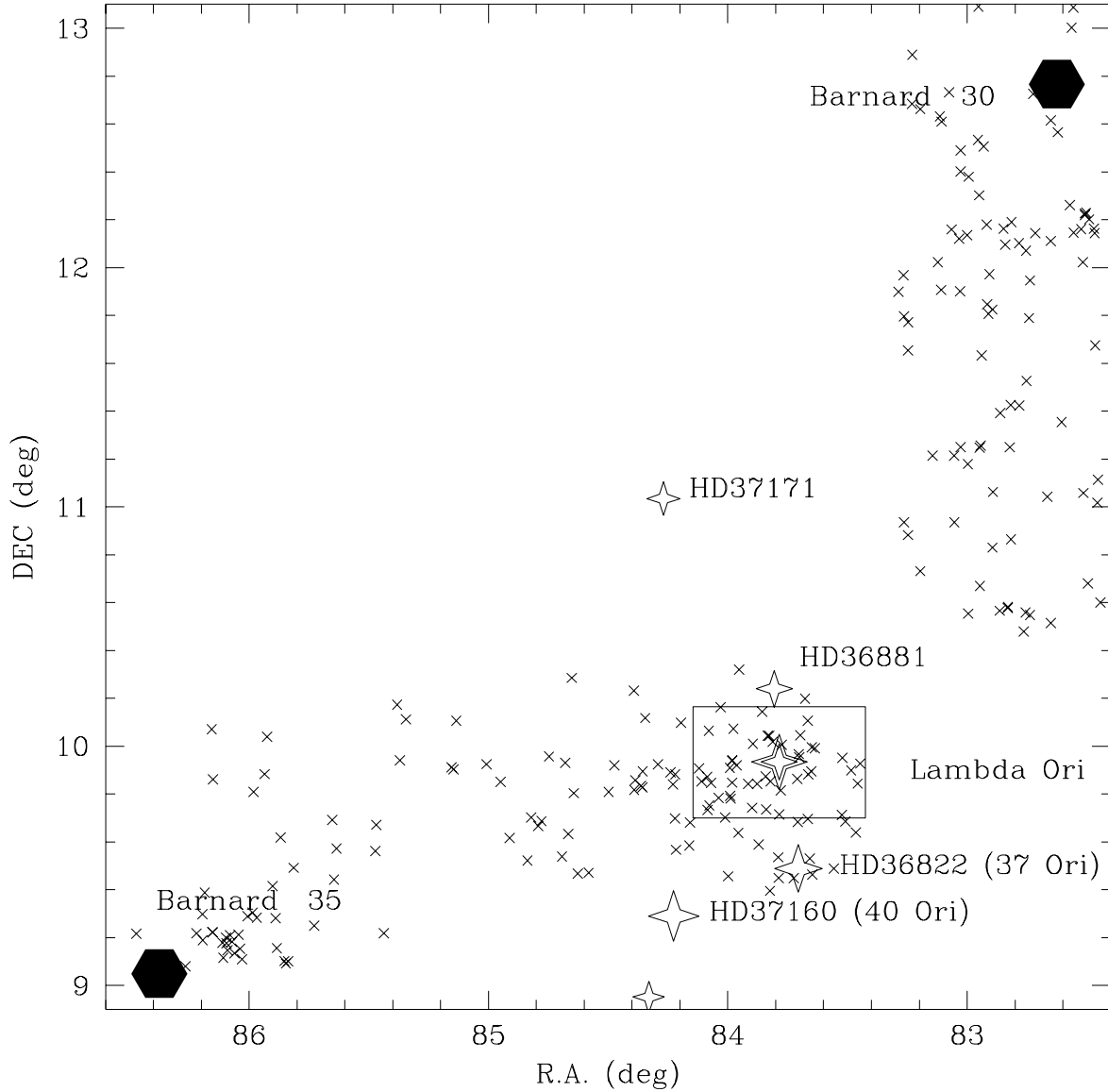


Fig. 1.— Location of our CFHT survey in the Cousins R and I filters (box). The location of the dark clouds Barnard 30 and Barnard 35 are indicated, as well as the stars listed in the Bright Star Catalog. Pre-main sequence stars identified by Dolan & Mathieu (1999, 2001) are displayed as crosses.

Table 1: Positions and optical photometric data for our lambda Orionis candidate members.

LOri CFHT #	R.A. (2000.0) (h:m:s)	DEC ($^{\circ}$ ' ")	Ic	(R-I)c	δR	δI	Ic	(R-I)c	δR	δI
			shallow exp.				deep exp.			
151	5:35:58.65	9:48:54.74	—	—	—	—	19.00	1.98	0.02	0.01
152	5:34:11.26	9:44:26.70	—	—	—	—	19.05	2.38	0.04	0.01
153	5:36:18.20	9:57:40.97	—	—	—	—	19.17	2.13	0.03	0.01
154	5:34:19.78	9:54:20.84	—	—	—	—	19.31	2.48	0.05	0.01
155	5:36:25.07	10:01:54.32	—	—	—	—	19.36	2.51	0.06	0.01
156	5:34:36.28	9:55:32.18	—	—	—	—	19.59	2.46	0.06	0.01
157	5:34:11.26	9:55:36.84	—	—	—	—	19.63	2.46	0.06	0.01
158	5:34:20.40	10:03:47.61	—	—	—	—	19.67	2.40	0.05	0.01
159	5:36:33.18	10:00:34.29	—	—	—	—	20.01	2.24	0.06	0.01
160	5:34:11.27	9:45:10.72	—	—	—	—	20.29	2.53	0.13	0.02
161	5:35:54.10	9:43:36.11	—	—	—	—	20.34	2.75	0.19	0.01
162	5:35:04.44	9:57:33.64	—	—	—	—	20.42	2.80	0.51	0.02
163	5:35:18.36	9:56:52.78	—	—	—	—	20.42	2.54	0.24	0.02
164	5:34:11.24	9:52:49.35	—	—	—	—	20.44	2.67	0.17	0.01
165	5:35:11.57	9:53:00.56	—	—	—	—	20.73	2.39	0.22	0.02
166	5:34:00.35	9:54:22.45	—	—	—	—	20.75	2.58	0.18	0.02
167	5:35:14.19	9:54:07.52	—	—	—	—	20.90	2.96	0.64	0.02
168	5:34:50.32	9:45:16.92	—	—	—	—	21.54	2.61	0.62	0.04
169	5:34:59.08	9:58:55.60	—	—	—	—	21.88	2.95	1.10	0.05
170	5:35:36.88	9:44:24.41	—	—	—	—	22.06	3.35	2.61	0.07

δR and δI correspond to the internal errors as computed with IRAF. For other sources of the photometric errors, see the text.

Table 2: Positions and IR photometry from 2MASS for our lambda Orionis candidate members.

LOri CFHT	Ic	dist	RA (2000.0)	DEC	J errorJ	H errorH	K error K	Selection†	Mem
001	12.52	0.49	05:33:47.21	+09:55:38.5	11.297 0.022	10.595 0.022	10.426 0.021	Y,Y,Y,Y,Y,-	Mem
002	12.64	0.06	05:36:10.36	+10:08:54.8	11.230 0.024	10.329 0.023	10.088 0.019	N,N,Y,Y,N,-	NM-
003	12.65	0.65	05:35:55.43	+09:56:30.9	11.416 0.023	10.725 0.022	10.524 0.023	Y,Y,Y,Y,Y,-	Mem
004	12.65	0.63	05:35:47.58	+09:45:50.0	11.359 0.022	10.780 0.023	10.548 0.021	Y,Y,Y,Y,Y,-	Mem
005	12.67	0.45	05:33:53.66	+09:43:08.4	11.378 0.022	10.549 0.022	10.354 0.023	N,N,Y,Y,N,-	NM-
006	12.75	0.87	05:35:16.23	+09:55:18.5	11.542 0.026	10.859 0.026	10.648 0.021	Y,Y,Y,Y,Y,-	Mem
007	12.78	0.51	05:34:29.53	+09:48:58.3	11.698 0.027	11.101 0.024	10.895 0.030	Y,Y,Y,Y,Y,-	Mem
008	12.79	0.16	05:35:57.98	+09:54:32.8	11.548 0.029	10.859 0.023	10.651 0.024	Y,Y,Y,Y,Y,-	Mem
009	12.95	0.26	05:34:46.35	+10:06:35.8	11.843 0.024	11.109 0.024	10.923 0.023	Y,Y,Y,Y,Y,-	Mem
010	12.96	0.11	05:34:32.97	+10:08:41.2	11.880 0.026	11.219 0.026	11.041 0.023	Y,Y,Y,Y,Y,-	Mem
011	13.01	0.51	05:34:44.66	+09:53:58.0	11.604 0.026	10.784 0.024	10.554 0.024	N,N,Y,Y,N,-	NM-
012	13.03	0.28	05:35:05.96	+09:52:08.0	11.816 0.026	10.971 0.024	10.795 0.023	N,Y,Y,Y,N,-	NM-
013	13.03	0.27	05:33:56.34	+09:53:56.9	11.656 0.022	10.918 0.022	10.719 0.023	Y,Y,Y,Y,Y,-	Mem
014	13.03	0.13	05:36:19.04	+10:03:50.9	11.941 0.024	11.278 0.027	11.092 0.023	Y,Y,Y,Y,Y,-	Mem
015	13.05	0.45	05:34:21.82	+10:04:14.9	11.870 0.024	11.127 0.024	10.912 0.019	Y,Y,Y,Y,Y,-	Mem
016	13.18	0.98	05:35:13.46	+09:55:25.3	11.958 0.024	11.284 0.027	11.053 0.024	Y,Y,Y,Y,Y,-	Mem
017	13.19	0.35	05:36:20.51	+09:52:19.2	12.188 0.024	11.482 0.023	11.323 0.021	Y,Y,Y,Y,Y,-	Mem
018	13.26	0.52	05:36:16.61	+09:50:48.4	11.991 0.024	11.284 0.022	11.090 0.023	Y,Y,Y,Y,Y,-	Mem
019	13.31	1.56	05:35:13.65	+09:56:27.3	12.019 0.026	11.316 0.024	11.067 0.021	Y,Y,Y,Y,Y,-	Mem
020	13.31	0.26	05:34:57.57	+09:46:07.2	11.856 0.028	11.214 0.026	11.025 0.027	Y,Y,Y,Y,Y,-	Mem
021	13.38	0.34	05:35:06.94	+09:48:57.5	12.258 0.027	11.560 0.026	11.296 0.021	Y,Y,Y,Y,Y,-	Mem
022	13.38	0.49	05:35:51.34	+09:55:11.2	12.102 0.023	11.411 0.022	11.156 0.019	Y,Y,Y,Y,Y,-	Mem
023	13.44	0.68	05:35:57.68	+09:47:34.1	12.221 0.027	11.471 0.022	11.290 0.024	Y,Y,Y,Y,Y,-	Mem
024	13.45	0.66	05:34:57.12	+09:54:36.7	12.139 0.030	11.446 0.026	11.223 0.028	Y,Y,Y,Y,Y,-	Mem
025	13.45	0.31	05:36:20.20	+09:44:01.9	12.163 0.044	11.409 0.051	11.090 0.033	N,Y,Y,Y,Y,-	Mem?
026	13.47	0.66	05:34:36.23	+09:53:44.2	12.046 0.028	11.324 0.024	11.092 0.025	Y,Y,Y,Y,Y,-	Mem
027	13.50	0.27	05:35:11.01	+10:07:36.4	12.378 0.026	11.718 0.023	11.503 0.021	Y,Y,Y,Y,Y,-	Mem
028	13.65	0.38	05:36:18.87	+09:51:35.1	12.488 0.024	11.872 0.022	11.687 0.021	N,Y,Y,Y,Y,-	Mem?
029	13.69	0.35	05:35:25.37	+10:08:38.4	12.210 0.026	11.460 0.027	11.071 0.019	N,N,Y,Y,Y,-	NM-
030	13.74	0.86	05:35:12.54	+09:55:19.5	12.427 0.027	11.686 0.026	11.428 0.021	Y,Y,Y,Y,Y,-	Mem
031	13.75	1.30	05:34:49.02	+09:58:02.1	12.412 0.028	11.654 0.023	11.442 0.028	Y,Y,Y,Y,Y,-	Mem
032	13.80	0.97	05:36:09.32	+09:47:02.7	12.410 0.029	11.714 0.023	11.493 0.021	Y,Y,Y,Y,Y,-	Mem
033	13.81	0.20	05:35:34.84	+10:00:35.3	12.455 0.033	11.800 0.042	11.502 0.027	Y,Y,Y,Y,Y,-	Mem
034	13.97	0.10	05:35:19.92	+10:02:36.5	12.442 0.026	11.639 0.026	11.184 0.023	N,N,Y,Y,Y,-	NM-
035	13.97	0.42	05:35:15.14	+10:01:06.8	12.546 0.024	11.842 0.027	11.609 0.019	Y,Y,Y,Y,Y,-	Mem
036	13.98	0.87	05:34:39.29	+10:01:28.7	12.576 0.024	11.936 0.023	11.706 0.021	Y,Y,Y,Y,Y,-	Mem
037	13.99	1.14	05:34:35.61	+09:59:43.3	12.459 0.024	11.727 0.026	11.492 0.021	Y,Y,Y,Y,Y,-	Mem
038	14.01	0.73	05:33:49.93	+09:50:36.8	12.684 0.030	11.954 0.029	011.752 -	Y,Y,Y,Y,Y,-	Mem
039	14.02	0.61	05:35:57.09	+09:46:52.6	12.755 0.030	12.004 0.023	11.775 0.023	Y,Y,Y,Y,Y,-	Mem
040	14.06	0.25	05:35:39.48	+09:50:32.8	12.553 0.024	11.877 0.022	11.594 0.024	Y,Y,Y,Y,Y,-	Mem
041	14.10	0.45	05:35:30.45	+09:50:34.1	12.500 0.024	11.856 0.023	11.587 0.027	Y,Y,Y,Y,Y,-	Mem
042	14.14	0.33	05:36:07.11	+10:09:47.7	12.813 0.027	12.099 0.026	11.853 0.023	Y,Y,Y,Y,Y,-	Mem
043	14.16	1.83	05:35:02.74	+09:56:47.6	12.707 0.024	12.021 0.026	11.741 0.024	Y,Y,Y,Y,Y,-	Mem
044	14.17	0.17	05:34:08.39	+09:51:25.3	12.924 0.024	12.318 0.024	12.065 0.023	Y,Y,Y,Y,Y,-	Mem
045	14.23	1.42	05:35:07.42	+09:58:22.4	12.768 0.023	12.102 0.026	11.844 0.023	Y,Y,Y,Y,Y,-	Mem
046	14.36	0.33	05:34:26.08	+09:51:49.4	13.033 0.023	12.478 0.026	12.252 0.026	N,Y,Y,Y,Y,-	Mem?
047	14.38	0.61	05:35:55.67	+09:50:53.3	12.732 0.026	12.097 0.031	11.827 0.026	Y,Y,Y,Y,Y,-	Mem
048	14.41	0.49	05:35:12.56	+09:53:11.1	12.887 0.027	12.196 0.029	11.932 0.026	Y,Y,Y,Y,Y,-	Mem
049	14.50	0.27	05:35:01.00	+09:49:36.1	13.173 0.027	12.592 0.029	12.253 0.023	Y,Y,Y,Y,Y,-	Mem
050	14.54	0.81	05:34:56.40	+09:55:04.6	12.877 0.027	12.236 0.027	11.955 0.031	Y,Y,Y,Y,Y,-	Mem

† Selection criteria: (1) [K,J-K]; (2) [I,I-K]; (3) [I-J,H-K]; (4) [I-J,I-K];(5) [J-H,H-K]; (6) Spectral type.

Table 2: Positions and IR photometry from 2MASS for our lambda Orionis candidate members.

L Ori CFHT	Ic	dist	RA (2000.0)	DEC	J errorJ	H errorH	K error K	Selection†	Mem
051	14.60	0.41	05:36:12.14	+10:00:57.0	13.266 0.024	12.559 0.022	12.285 0.021	Y,Y,Y,Y,Y,-	Mem
052	14.63	0.55	05:34:11.78	+09:57:03.4	13.117 0.023	12.454 0.024	12.192 0.019	Y,Y,Y,Y,Y,-	Mem
053	14.72	0.34	05:34:36.73	+09:52:58.3	13.173 0.032	12.521 0.023	12.278 0.027	Y,Y,Y,Y,Y,-	Mem
054	14.73	0.74	05:35:52.55	+09:48:31.1	13.189 0.024	12.509 0.022	12.271 0.027	Y,Y,Y,Y,Y,-	Mem
055	14.76	0.30	05:35:21.43	+09:49:56.6	13.184 0.026	12.477 0.026	12.253 0.026	Y,Y,Y,Y,Y,-	Mem
056	14.87	0.44	05:34:58.37	+09:53:47.1	13.211 0.029	12.567 0.026	12.267 0.029	Y,Y,Y,Y,Y,-	Mem
057	15.04	0.74	05:35:11.32	+10:00:50.2	13.412 0.024	12.773 0.023	12.487 0.030	Y,Y,Y,Y,Y,-	Mem
058	15.06	0.71	05:36:10.36	+10:00:18.4	13.521 0.024	12.935 0.022	12.643 0.027	Y,Y,Y,Y,Y,-	Mem
059	15.10	0.28	05:34:23.55	+09:43:43.4	13.574 0.026	12.884 0.026	12.682 0.032	Y,Y,Y,Y,Y,-	Mem
060	15.14	0.38	05:35:20.00	+09:49:06.2	13.598 0.030	12.961 0.030	12.663 0.029	Y,Y,Y,Y,Y,-	Mem
061	15.15	0.15	05:35:18.18	+09:52:24.2	13.533 0.023	12.833 0.026	12.525 0.027	Y,Y,Y,Y,Y,-	Mem
062	15.16	0.35	05:35:15.33	+09:48:37.0	13.634 0.029	13.005 0.030	12.725 0.027	Y,Y,Y,Y,Y,-	Mem
063	15.34	0.60	05:35:19.14	+09:54:42.4	13.756 0.029	13.066 0.029	12.663 0.030	N,Y,Y,Y,Y,-	Mem?
064	15.34	0.49	05:35:52.01	+09:50:29.4	13.782 0.026	13.098 0.025	12.846 0.029	Y,Y,Y,Y,Y,-	Mem
065	15.37	1.27	05:35:17.92	+09:56:57.2	13.820 0.024	13.123 0.029	12.843 0.027	Y,Y,Y,Y,Y,-	Mem
066	15.40	1.72	05:35:06.78	+09:57:27.8	13.506 0.024	12.901 0.026	12.654 0.029	Y,Y,Y,Y,Y,-	Mem
067	15.53	0.18	05:36:26.38	+09:45:46.6	14.000 0.033	13.356 0.027	13.102 0.036	Y,Y,Y,Y,Y,-	Mem
068	15.20	0.44	05:34:48.02	+09:43:26.2	13.521 0.027	12.902 0.026	12.628 0.027	Y,N,Y,Y,Y,-	Mem?
069	15.20	0.21	05:34:43.97	+09:48:35.6	13.384 0.027	12.774 0.027	12.425 0.027	Y,N,Y,Y,Y,-	Mem?
070	15.61	0.34	05:36:00.01	+10:05:48.8	14.042 0.032	13.405 0.029	13.067 0.031	Y,Y,Y,Y,Y,-	Mem
071	15.45	0.26	05:34:15.79	+10:06:54.6	13.749 0.030	13.129 0.024	12.839 0.031	Y,Y,Y,Y,Y,-	Mem
072	15.35	1.93	05:34:11.41	+09:42:07.9	13.554 0.026	12.944 0.032	12.631 0.027	Y,N,Y,Y,Y,-	Mem?
073	15.28	0.02	05:34:46.82	+09:50:37.9	13.644 0.028	12.992 0.023	12.715 0.027	Y,N,Y,Y,Y,-	Mem?
074	15.39	0.93	05:36:00.54	+09:42:39.0	13.663 0.026	13.088 0.025	12.720 0.024	Y,N,Y,Y,Y,-	Mem?
075	15.23	0.61	05:34:55.22	+10:00:34.7	13.396 0.026	12.794 0.026	12.526 0.024	Y,N,N,Y,Y,Y	Mem?
076	15.81	1.29	05:35:10.96	+09:57:43.8	14.216 0.027	13.527 0.027	13.201 0.032	Y,Y,Y,Y,Y,-	Mem
077	15.89	1.07	05:34:41.72	+09:42:42.0	14.031 0.027	13.416 0.027	13.109 0.035	Y,Y,Y,Y,Y,-	Mem
078	15.92	0.62	05:36:16.45	+09:50:15.9	14.227 0.041	13.593 0.053	13.286 0.040	Y,Y,Y,Y,Y,-	Mem
079	16.00	0.76	05:34:48.26	+09:59:53.9	14.221 0.032	13.536 0.032	13.338 0.039	Y,Y,N,Y,Y,-	Mem?
080	16.01	0.34	05:35:30.05	+09:59:25.5	13.804 0.023	13.196 0.022	12.891 0.033	Y,N,Y,Y,Y,-	Mem?
081	16.02	0.43	05:33:56.61	+10:06:14.9	14.669 0.032	13.692 0.032	13.209 0.037	Y,Y,Y,Y,Y,Y	Mem+
082	16.02	0.34	05:36:00.81	+09:52:57.1	14.200 0.033	13.570 0.025	13.281 0.033	Y,Y,Y,Y,Y,Y	Mem+
083	16.02	0.67	05:35:43.41	+09:54:26.8	14.265 0.030	13.638 0.035	13.375 0.040	Y,Y,Y,Y,Y,-	Mem
084	16.03	1.19	05:35:50.80	+10:09:45.2	14.077 0.024	13.448 0.027	13.188 0.034	Y,Y,Y,Y,Y,-	Mem
085	16.04	0.38	05:35:21.52	+09:53:29.2	14.189 0.026	13.622 0.037	13.233 0.027	Y,Y,Y,Y,Y,-	Mem
086	16.09	0.67	05:34:11.58	+09:49:15.0	14.482 0.032	13.867 0.032	13.503 0.040	Y,Y,Y,Y,Y,-	Mem
087	16.09	1.03	05:34:33.77	+09:55:34.2	14.186 0.039	13.601 0.030	13.279 0.035	Y,Y,Y,Y,Y,Y	Mem+
088	16.10	1.07	05:34:49.50	+09:58:46.8	14.140 0.031	13.543 0.037	13.228 0.039	Y,Y,Y,Y,Y,-	Mem
089	16.15	0.15	05:35:04.00	+10:07:26.8	14.380 0.032	13.839 0.035	13.512 0.039	Y,Y,Y,Y,Y,-	Mem
090	16.17	0.48	05:36:27.08	+09:51:34.7	14.515 0.041	13.881 0.023	13.651 0.051	Y,Y,Y,Y,Y,-	Mem
091	16.18	0.76	05:34:35.86	+09:54:26.5	14.184 0.032	13.556 0.032	13.289 0.031	Y,Y,Y,Y,Y,-	Mem
092	16.19	0.50	05:35:50.97	+09:51:03.5	14.441 0.030	13.841 0.038	13.537 0.040	Y,Y,Y,Y,Y,-	Mem
093	16.21	0.15	05:34:41.20	+09:50:16.3	14.462 0.030	13.836 0.039	13.604 0.052	Y,Y,Y,Y,Y,-	Mem
094	16.28	0.19	05:34:43.17	+10:01:59.8	14.404 0.034	13.802 0.030	13.425 0.038	Y,Y,Y,Y,Y,-	Mem
095	16.35	0.64	05:35:24.18	+09:55:15.4	14.564 0.033	13.913 0.029	13.613 0.048	Y,Y,Y,Y,Y,Y	Mem+
096	16.37	1.45	05:35:11.13	+09:57:19.6	14.627 0.038	13.965 0.037	13.638 0.047	Y,Y,Y,Y,Y,-	Mem
098	16.40	0.52	05:36:31.50	+09:45:01.7	14.647 0.037	13.985 0.045	13.682 0.039	Y,Y,Y,Y,Y,Y	Mem+
099	16.42	0.28	05:34:45.59	+10:05:48.9	14.709 0.034	14.074 0.035	13.676 0.043	Y,Y,Y,Y,Y,-	Mem
100	16.43	0.39	05:35:00.10	+09:46:14.0	14.768 0.044	14.044 0.042	13.821 0.044	Y,Y,Y,Y,Y,-	Mem

† Selection criteria: (1) [K,J-K]; (2) [I,I-K]; (3) [I-J,H-K]; (4) [I-J,I-K]; (5) [J-H,H-K]; (6) Spectral type.

Table 2: Positions and IR photometry from 2MASS for our lambda Orionis candidate members.

LOri CFHT	Ic	dist	RA (2000.0)	DEC	J errorJ	H errorH	K error K	Selection†	Mem
101	16.48	1.79	05:36:30.41	+10:08:54.3	15.019 0.038	14.372 0.044	14.110 0.066	Y,N,Y,Y,Y, -	Mem?
102	16.50	0.31	05:35:22.02	+09:52:52.3	14.634 0.047	14.083 0.050	13.809 0.057	N,Y,Y,Y,Y, -	Mem?
103	16.55	0.19	05:35:22.56	+09:45:01.9	14.643 0.029	14.126 0.029	13.833 0.055	N,Y,Y,Y,Y, -	Mem?
104	16.71	0.52	05:35:07.07	+09:54:01.5	14.667 0.030	14.136 0.036	13.721 0.042	Y,Y,Y,Y,Y, -	Mem
105	16.75	0.46	05:34:17.58	+09:52:29.7	14.922 0.040	14.340 0.052	13.993 0.053	Y,Y,Y,Y,Y, -	Mem
106	16.76	0.46	05:35:28.77	+09:54:10.2	14.776 0.043	14.161 0.057	13.743 0.045	Y,Y,Y,Y,Y, -	Mem
107	16.78	0.46	05:35:55.19	+09:52:20.0	14.656 0.036	13.987 0.035	13.621 0.052	Y,Y,Y,Y,Y, Y	Mem+
108	16.80	0.26	05:35:26.04	+10:08:09.8	14.840 0.033	14.256 0.048	13.918 0.050	Y,Y,Y,Y,Y, -	Mem
109	16.81	0.04	05:34:08.54	+09:50:43.5	15.023 0.047	14.376 0.043	14.087 0.064	Y,Y,Y,Y,Y, -	Mem
110	16.82	0.36	05:35:32.61	+09:52:48.7	15.043 0.051	14.475 0.056	14.144 0.060	Y,Y,Y,Y,Y, Y	Mem+
111	16.86	0.46	05:34:19.57	+10:09:08.5	14.801 0.038	14.165 0.043	13.786 0.051	Y,Y,Y,Y,Y, -	Mem
112	16.87	0.57	05:34:33.53	+09:43:55.5	14.991 0.042	14.358 0.048	14.148 0.062	N,Y,N,Y,Y, -	NM-
113	16.99	0.11	05:33:47.91	+10:01:39.7	15.162 0.048	14.576 0.060	14.268 0.082	Y,Y,Y,Y,Y, -	Mem
114	17.06	0.18	05:36:18.11	+09:52:25.4	15.092 0.044	14.389 0.053	14.006 0.064	Y,Y,Y,Y,Y, Y	Mem+
115	17.08	0.14	05:34:46.32	+10:02:31.9	15.449 0.047	14.821 0.068	14.594 0.104	N,N,Y,Y,Y, N	NM+
116	17.17	0.72	05:35:12.03	+10:01:04.3	15.343 0.057	14.573 0.055	14.411 0.082	Y,Y,N,Y,N, Y	Mem+
118	17.23	0.31	05:35:24.41	+09:53:51.9	15.269 0.044	14.686 0.064	14.181 0.057	Y,Y,Y,Y,N, Y	Mem+
119	17.30	1.02	05:34:19.50	+09:42:23.7	14.760 -	14.262 -	14.548 0.106	N,Y,N,N,N, ?	NM?
120	17.34	0.78	05:34:46.21	+09:55:37.7	15.335 0.050	14.770 0.059	14.337 0.087	Y,Y,Y,Y,Y, -	Mem+
121	17.37	0.66	05:34:34.34	+09:42:17.1	15.533 0.060	15.093 0.086	14.748 0.099	N,N,Y,Y,N, -	NM-
122	17.38	0.13	05:34:35.44	+09:51:18.6	15.428 0.066	14.852 0.060	14.462 0.080	Y,Y,Y,Y,Y, -	Mem
124	17.45	0.67	05:34:14.25	+09:48:26.3	15.661 0.073	15.059 0.082	14.778 0.112	Y,N,Y,Y,Y, Y	Mem?
125	17.51	0.60	05:34:14.25	+09:48:26.3	15.661 0.073	15.059 0.082	14.778 0.112	N,N,Y,Y,Y, -	NM-
126	17.52	0.66	05:35:39.85	+09:53:24.1	15.511 0.077	14.911 0.096	14.335 -	Y,Y,Y,Y,N, Y	Mem+
127	17.53	1.31	05:34:11.18	+09:51:30.1	13.016 0.023	12.606 0.027	12.468 0.024	N,N,N,i,N, -	NM-
128	17.58	1.55	05:35:06.31	+09:58:01.3	15.624 0.077	15.099 0.087	14.769 0.109	N,Y,Y,Y,Y, -	Mem?
129	17.59	0.56	05:36:09.81	+09:42:37.0	15.383 0.056	14.816 0.072	14.526 0.102	N,Y,Y,Y,Y, -	Mem?
130	17.63	0.57	05:34:56.54	+09:42:33.0	15.731 0.059	15.265 0.092	14.735 0.110	Y,Y,Y,Y,N, Y	Mem+
131	17.78	0.47	05:36:06.99	+09:52:51.5	15.429 0.054	14.900 0.063	14.380 0.090	Y,Y,Y,Y,N, -	Mem?
132	17.82	0.59	05:34:29.16	+09:47:07.2	15.583 0.067	14.962 0.078	14.913 0.145	N,Y,N,Y,N, -	NM-
133	17.83	0.55	05:36:13.95	+10:08:10.1	16.290 0.101	15.900 0.167	15.378 0.203	N,N,Y,Y,N, N	NM+
134	17.90	0.59	05:35:22.85	+09:55:07.1	15.543 0.057	14.937 0.074	14.666 0.107	N,Y,N,Y,Y, N	NM+
135	17.90	0.39	05:35:09.33	+09:52:44.2	15.671 0.072	15.082 0.087	14.908 0.138	N,Y,N,Y,Y, Y	Mem?
136	17.92	1.69	05:34:38.37	+09:58:11.6	15.560 0.085	14.828 0.090	14.576 0.108	Y,Y,N,Y,Y, -	Mem?
138	17.96	0.59	05:33:43.48	+09:45:22.9	15.821 0.078	15.204 0.083	14.971 0.133	N,Y,N,Y,Y, -	NM-
139	18.16	0.25	05:35:44.34	+10:05:54.4	16.074 0.096	15.205 0.098	14.729 0.103	Y,Y,Y,Y,N, Y	Mem+
140	18.21	0.56	05:34:19.27	+09:48:27.5	15.981 0.078	15.224 0.089	14.750 0.113	Y,Y,Y,Y,Y, -	Mem+
141	18.25	0.31	05:35:38.06	+09:51:05.2	16.667 0.165	15.707 0.149	15.351 0.203	Y,N,Y,Y,N, N	NM+
142	18.27	0.57	05:34:17.01	+10:06:17.0	16.174 0.100	15.579 0.131	15.029 0.131	Y,Y,Y,Y,N, -	Mem?
143	18.30	1.30	05:35:00.95	+09:58:20.3	15.938 0.081	15.446 0.110	14.949 0.134	Y,Y,Y,Y,N, Y	Mem+
146	18.60	0.22	05:35:00.16	+09:52:40.9	16.230 0.107	15.470 0.110	14.936 0.128	Y,Y,Y,Y,Y, -	Mem
147	18.60	0.74	05:35:06.26	+09:46:53.8	16.833 0.178	16.531 0.286	15.689 0.255	Y,N,Y,Y,N, N	NM+
148	18.62	1.04	05:36:28.96	+09:43:22.3	16.545 0.154	15.783 0.152	15.709 0.244	N,N,N,Y,N, -	NM-
150	19.00	0.80	05:35:07.50	+09:49:32.9	16.656 0.152	16.134 0.197	15.560 0.214	Y,Y,Y,Y,N, Y	Mem+
152	19.05	0.56	05:34:11.30	+09:44:26.9	16.773 0.173	16.657 0.295	15.870 0.285	N,N,Y,Y,N, -	NM-
154	19.31	0.45	05:34:19.81	+09:54:20.6	16.804 0.169	16.143 0.192	15.513 0.219	Y,Y,Y,Y,N, Y	Mem+
155	19.36	0.35	05:36:25.05	+10:01:54.4	16.592 0.144	15.742 -	15.043 -	Y,Y,Y,Y,Y, Y	Mem+

† Selection criteria: (1) [K,J-K]; (2) [I,I-K]; (3) [I-J,H-K]; (4) [I-J,I-K];(5) [J-H,H-K]; (6) Spectral type.

Table 3: Spectroscopic data.

L Ori-CFHT #	Sp.Type	W(Ha) error (Å)	Member?
075	M5.0	9.4 0.5	Mem?
081	M5.5	4.2 0.4	Mem+
082	M4.5	8.6 0.8	Mem+
087	M4.5	6.7 0.4	Mem+
095	M6.0	7.3 0.6	Mem+
098	M5.0	12.9 3.1	Mem+
107	M6.0	11.7 1.3	Mem+
110	M5.5	9.1 1.6	Mem+
114	M6.5	10.9 0.9	Mem+
115	M5.0	8.5 0.4	NM+
116	M5.5	11.1 0.6	Mem+
117	M6.0	22.9 2.6	Mem+
118	M5.5	10.1 0.8	Mem+
119	M5.5	--	NM?
120	M5.5	7.4 1.1	Mem+
124	M5.5	8.4 0.4	Mem?
126	M6.5	26.2 1.9	Mem+
130	M5.5	8.7 0.7	Mem+
133	M4.5	1.9 0.4	NM+
134	M5.0	5.9 0.5	NM+
135	M7.0	15.5 1.7	Mem?
139	M6.0	19.7 1.2	Mem+
140	M7.0	72.8 4.2	Mem+
141	M4.5	4.3 0.2	NM+
143	M6.5	35.7 5.2	Mem+
147	M5.5	10.7 0.9	NM+
150	M8.0	15.6 1.5	Mem+
151	M5.5	11.6 1.0	NM?
154	M8.0	16.9 2.2	Mem+
155	M8.0	38. 15.	Mem+
156	M8.0	101.7 7.9	Mem+
161	M8.5	123. 56.	Mem+
165	M7.5†	16. 15.	NM?

† Due to te low S/N, the uncertainty in the spectral type classification is the one subclass, compared with half for the rest of the sample.

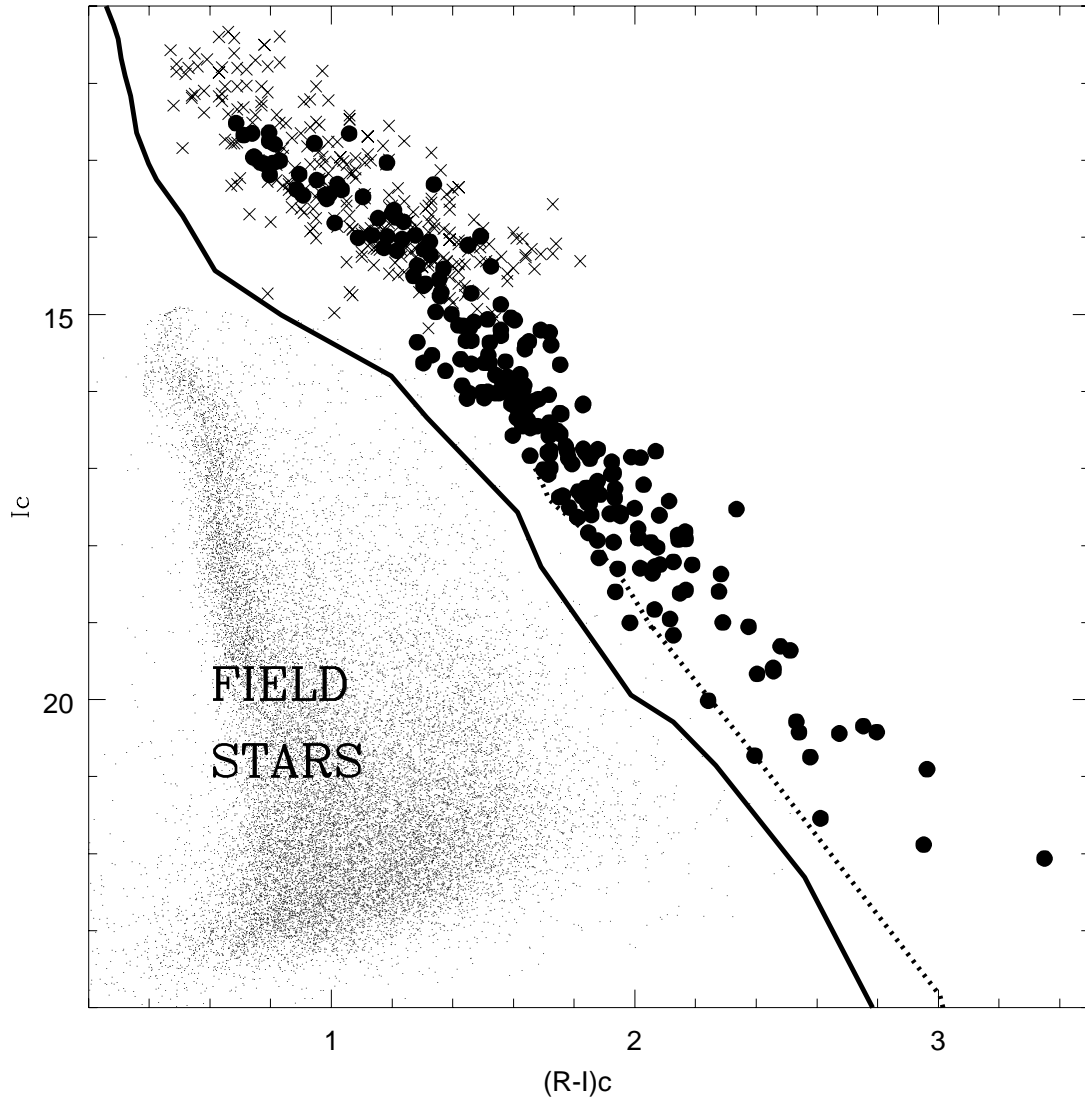


Fig. 2.— Optical color-magnitude diagram for the field around the λ Orionis star. Field stars are displayed as dots, previously known cluster members, brighter than the present survey, appear as crosses (Dolan & Mathieu 1999, 2001), whereas the new candidate members are included as solid circles. The thick, dotted line corresponds to Baraffe et al. (1998) 5 Myr isochrone, extended toward the red end using a NextGen model. The thick, solid line represent an empirical ZAMS (see Barrado y Navascués et al. 2001).

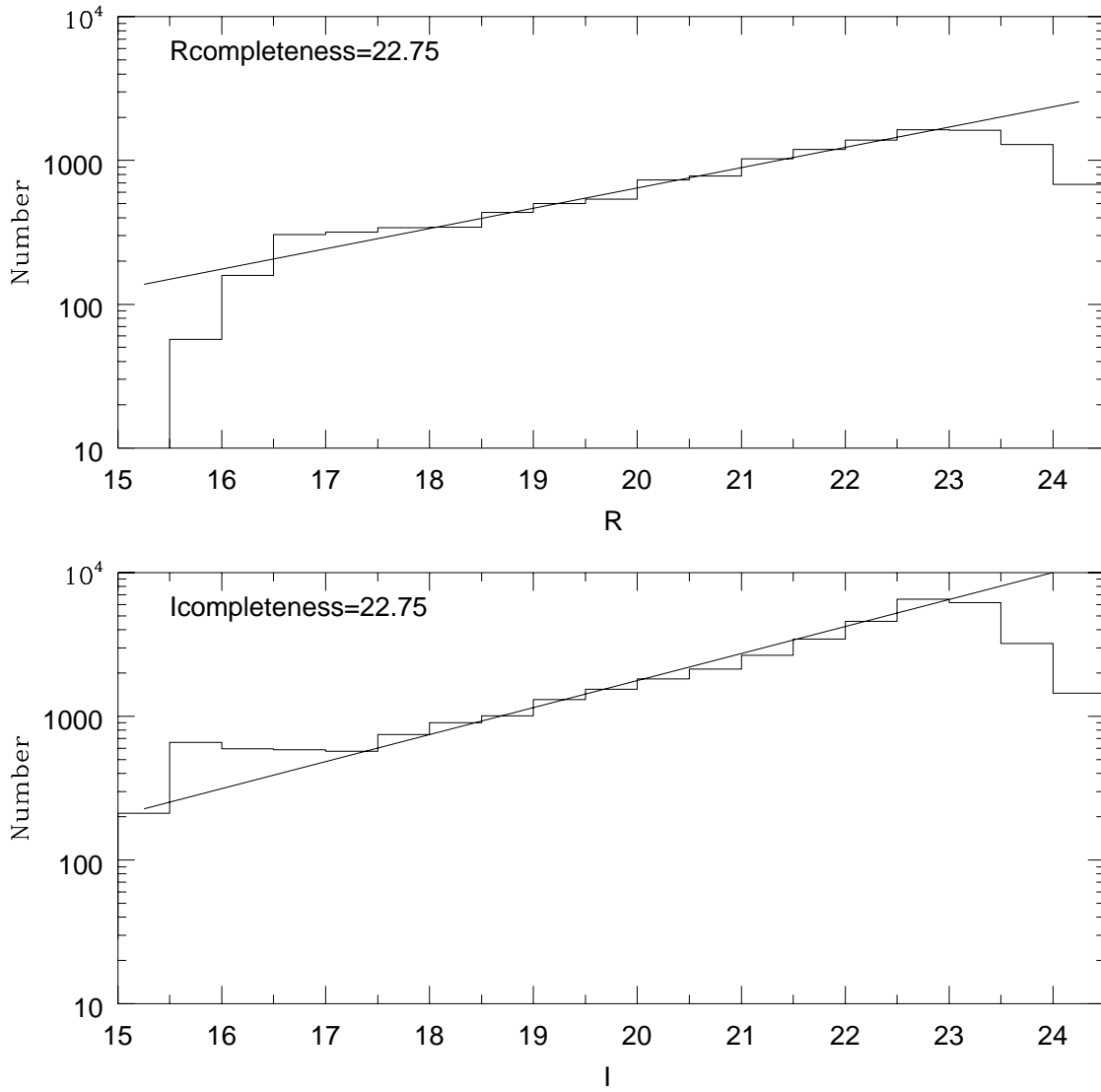


Fig. 3.— Completeness for the survey. For cluster members, the completeness limits are at $I(\text{complete})=20.2$ mag.

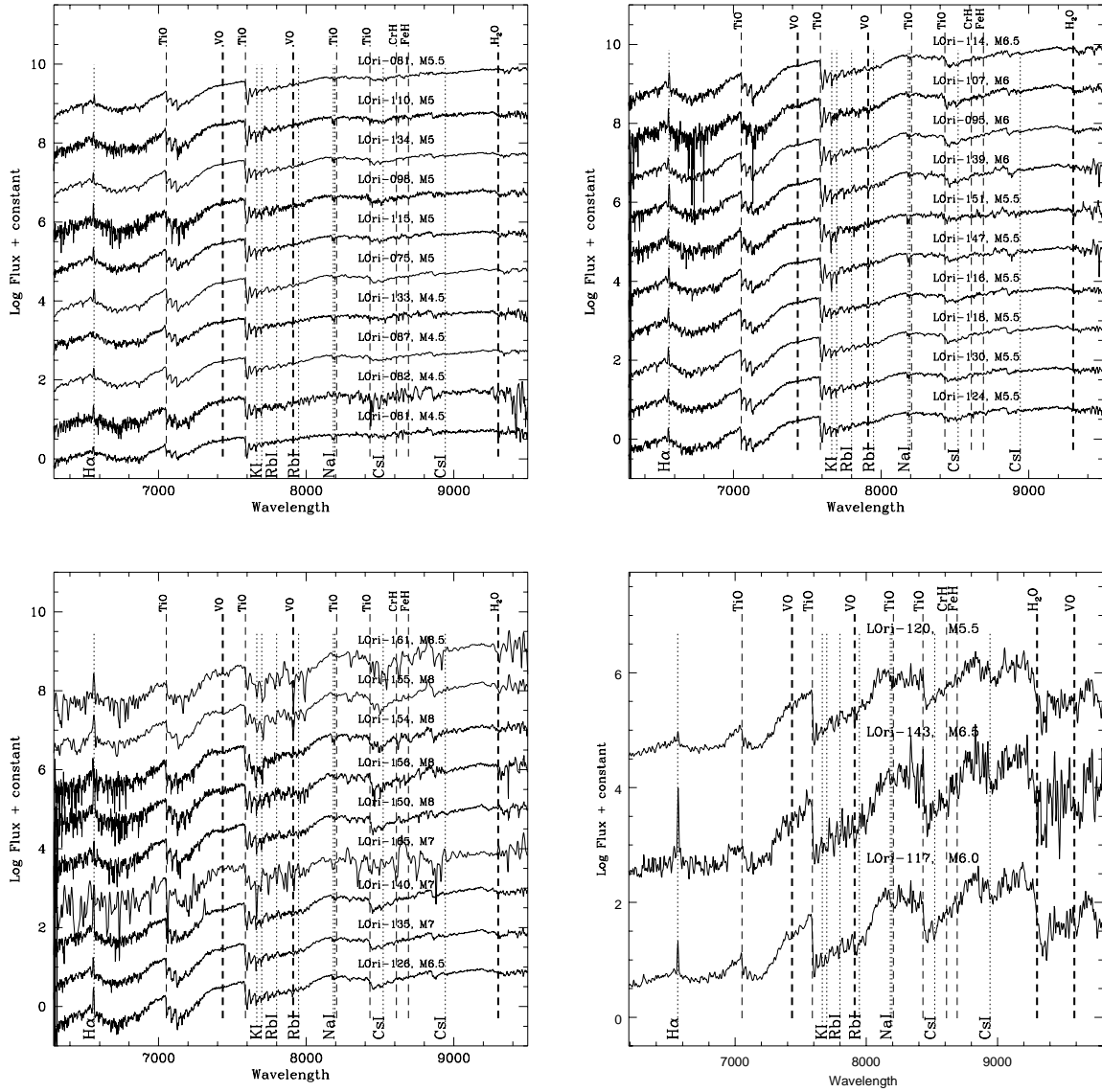


Fig. 4.— a, b and c Keck LRIS 400 l/mm spectra. d Magellan B&C 300 l/mm spectra.

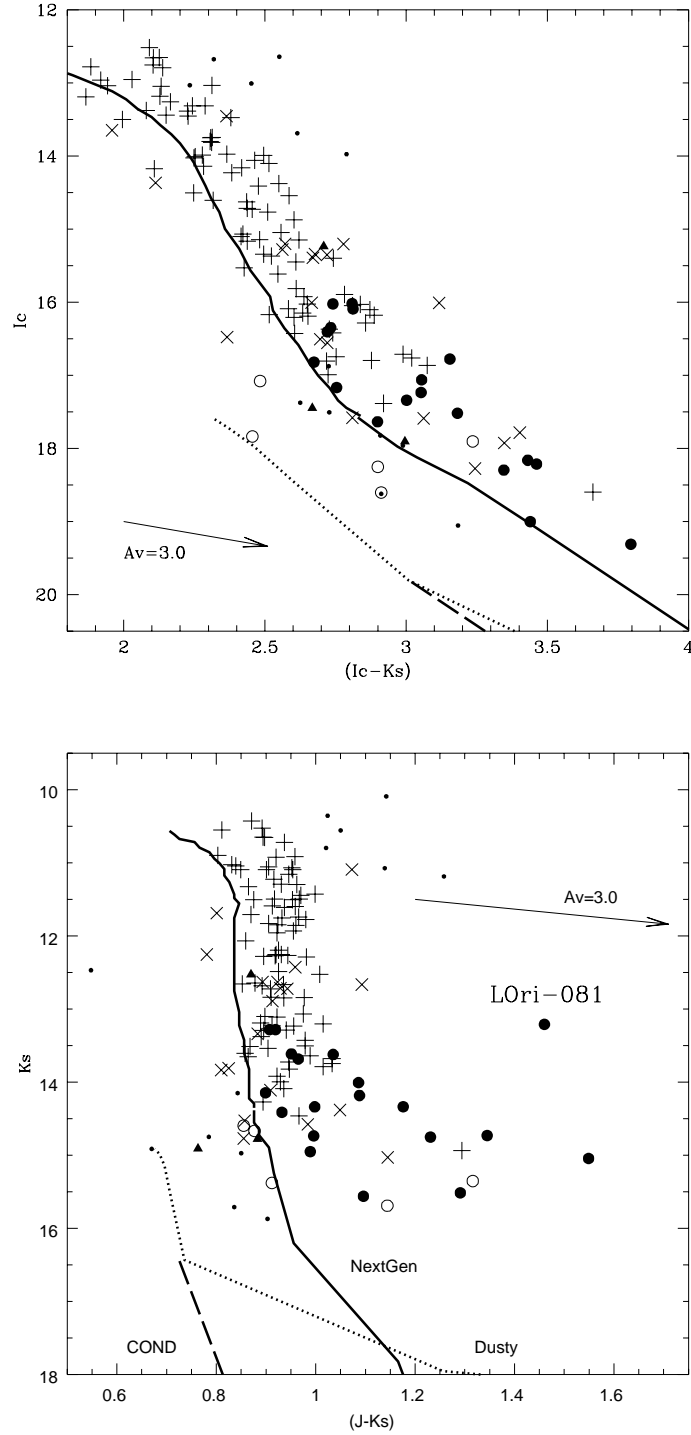


Fig. 5.— Color-magnitude diagram for Lambda Orionis candidate members. Those members without spectroscopy are displayed as: dots for "NM-", crosses for "Mem?", plus symbols for "mem". Candidates with low resolution spectroscopy appear as: open circles for "NM+", open triangles for "NM?", solid triangles for "Mem?", and solid circles for "Mem+". "NextGen", "Dusty" and "COND" models -5Myr isochrones from Baraffe et al. (1998, 2002) and Chabrier et al. (2000)– are included as solid, dotted and dashed lines, respectively.

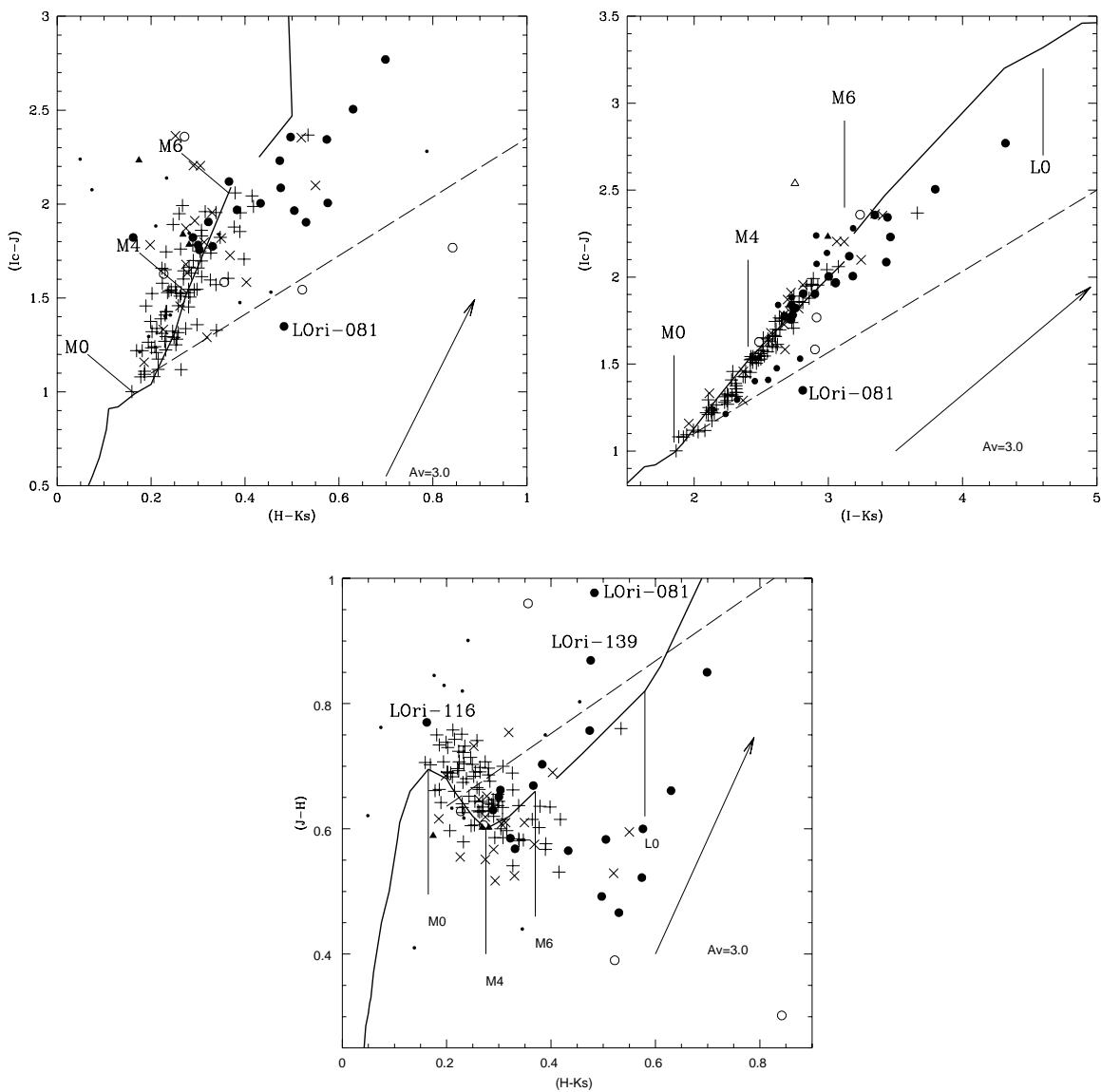


Fig. 6.— Optical-Infrared color-color diagram for Lambda Orionis candidate members. Those members without spectroscopy are displayed as: dots for "NM-", crosses for "Mem?", plus symbols for "mem". Candidates with low resolution spectroscopy appear as: open circles for "NM+", open triangles for "NM?", solid triangles for "Mem?", and solid circles for "Mem+". The thick-solid and dashed lines correspond to the locii of the main sequence stars (from Bessell & Brett 1988; Kirkpatrick et al. 2000; Leggett et al. 2001) and CTT stars (Meyer et al. 1997; Barrado y Navascués et al. 2003), respectively.

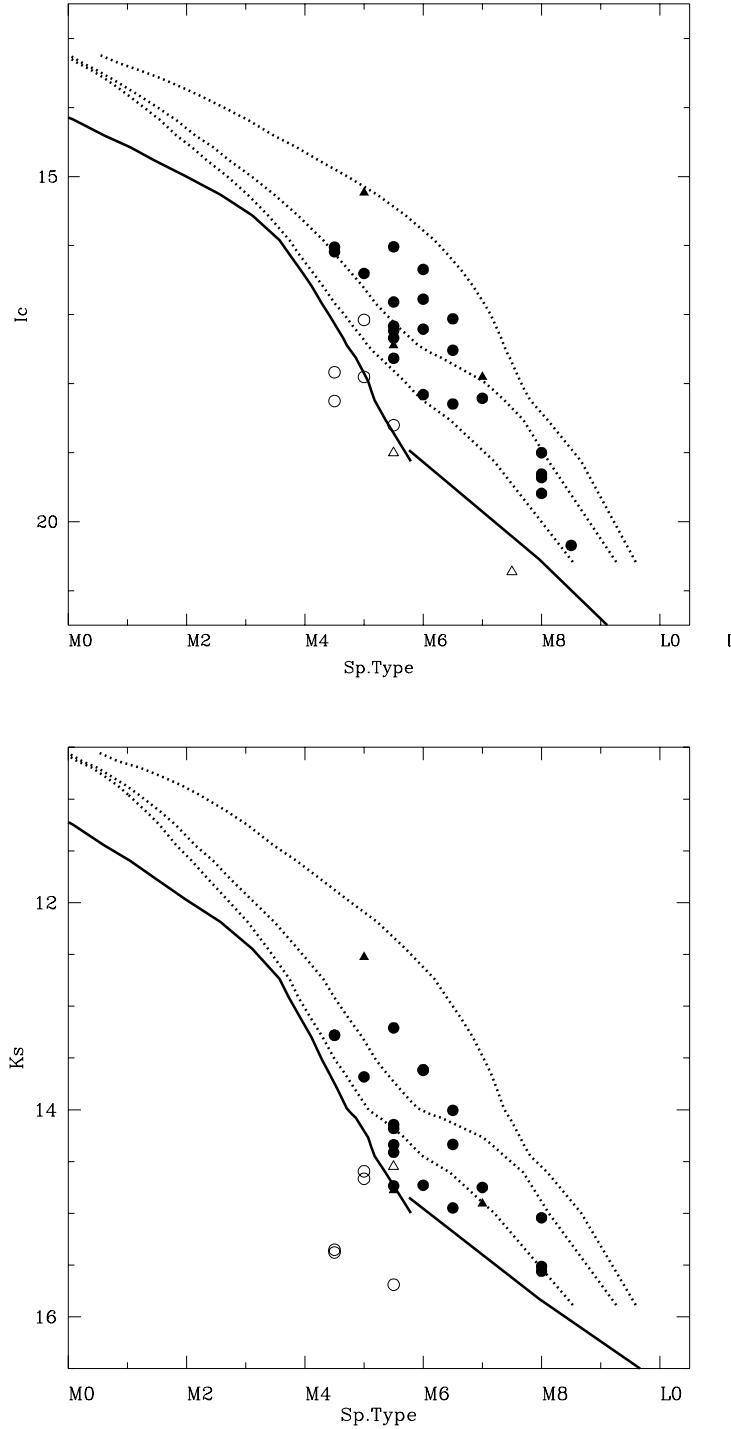


Fig. 7.— **a** I_c magnitude versus the spectral type. Symbols as in figure 5. The isochrones –5 Myr– correspond to models by Baraffe et al. (1998), after applying different temperature scales (Basri et al. 2000, solid line; Luhman 1999, dotted lines for different gravities). **b** K_s magnitude versus the spectral type. Symbols as in figure 5. The isochrones correspond to models by Baraffe et al. (1998), after applying different temperature scales (Basri et al. 2000, solid line; Luhman 1999, dotted lines for different gravities).

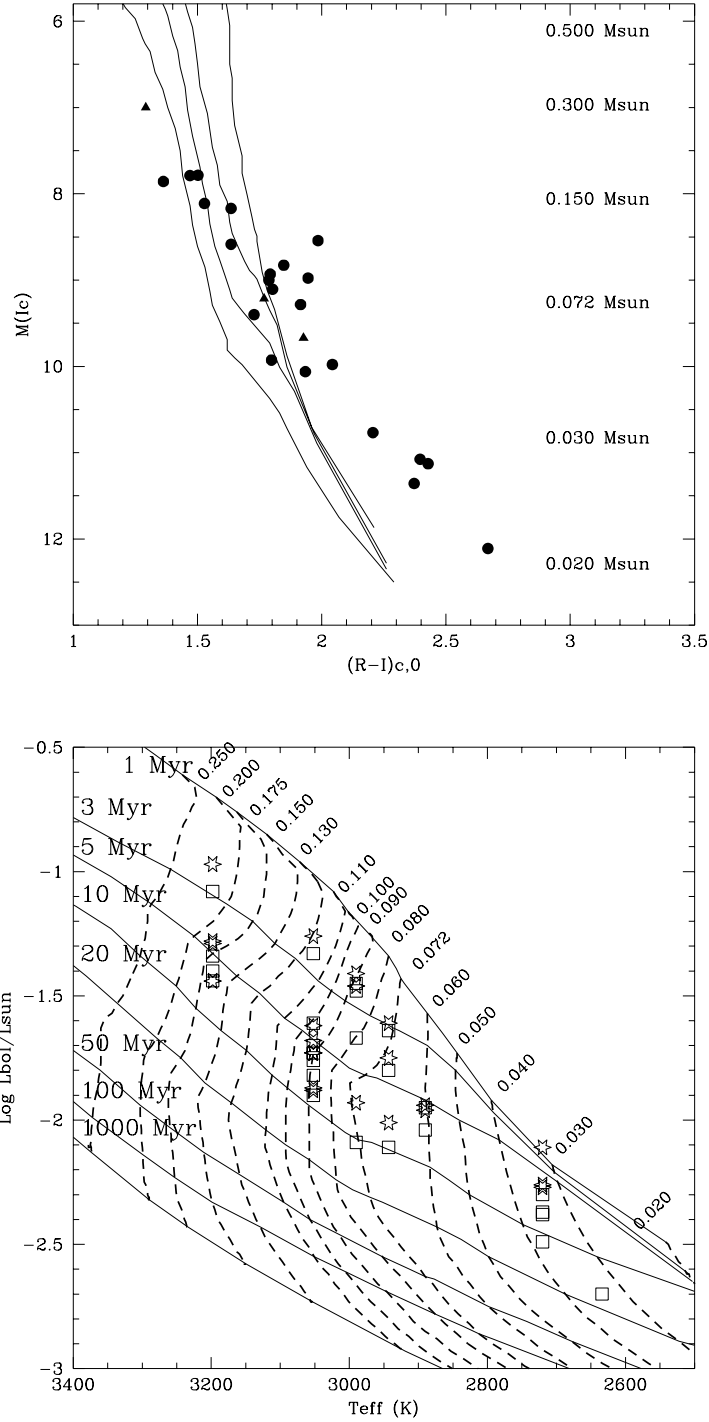


Fig. 8.— **a** Dereddened color versus the absolute magnitude for Lambda Orionis candidate members –subsample with low resolution spectroscopy. The thin lines correspond to Baraffe et al. (1998) 1, 3, 5 and 10 Myr isochrones. Solid circles correspond to probable members, solid triangle to possible (“Mem+” and “Mem?”, respectively). **b** Hertzsprung-Russell diagram for Lambda Orionis cluster probable and possible members –subsample with low resolution spectroscopy. Open squares and stars correspond to bolometric luminosities derived with Ic and Ks magnitudes (see text).

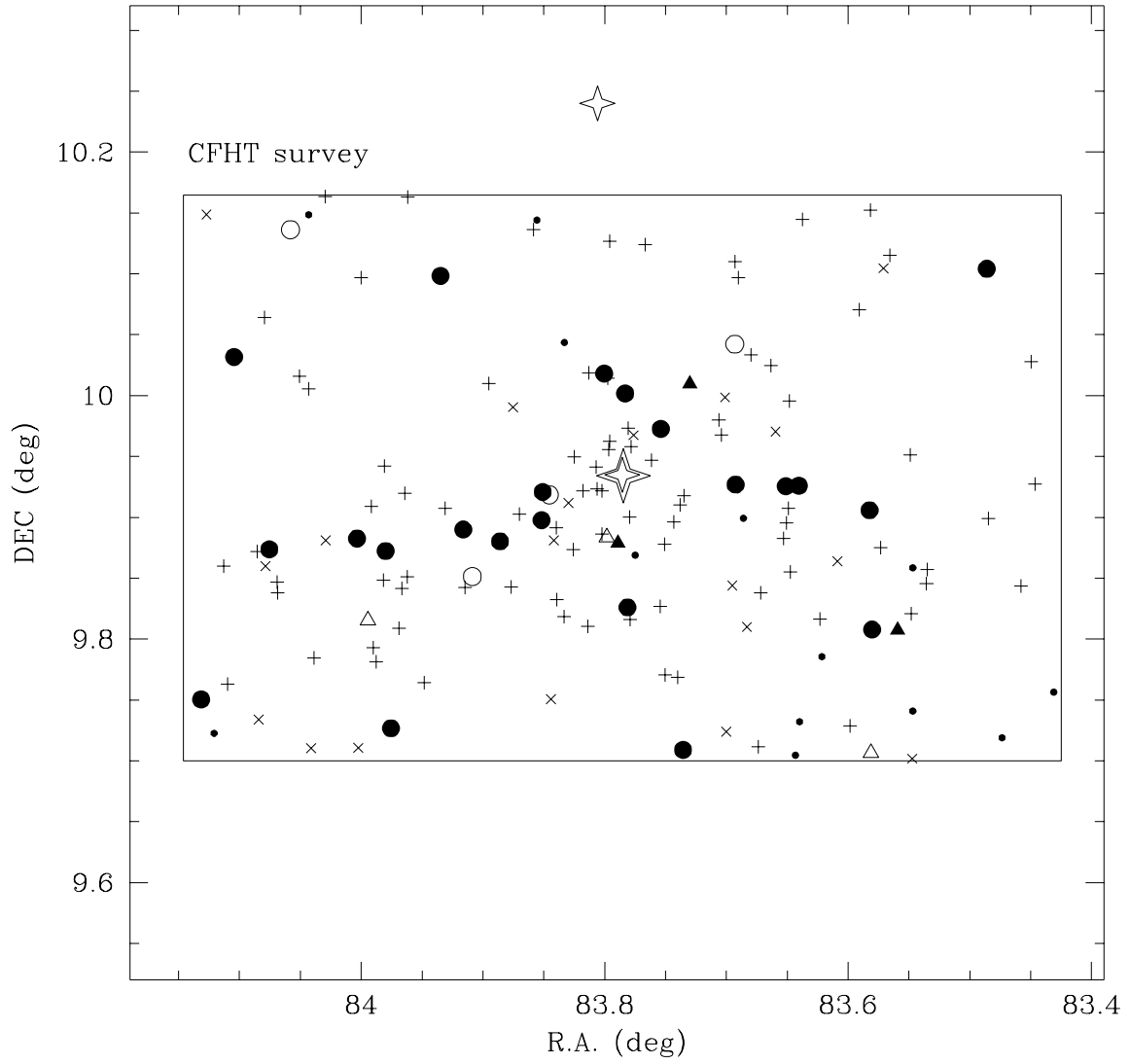


Fig. 9.— Spatial distribution of our candidate members. Symbols as in figure 5.

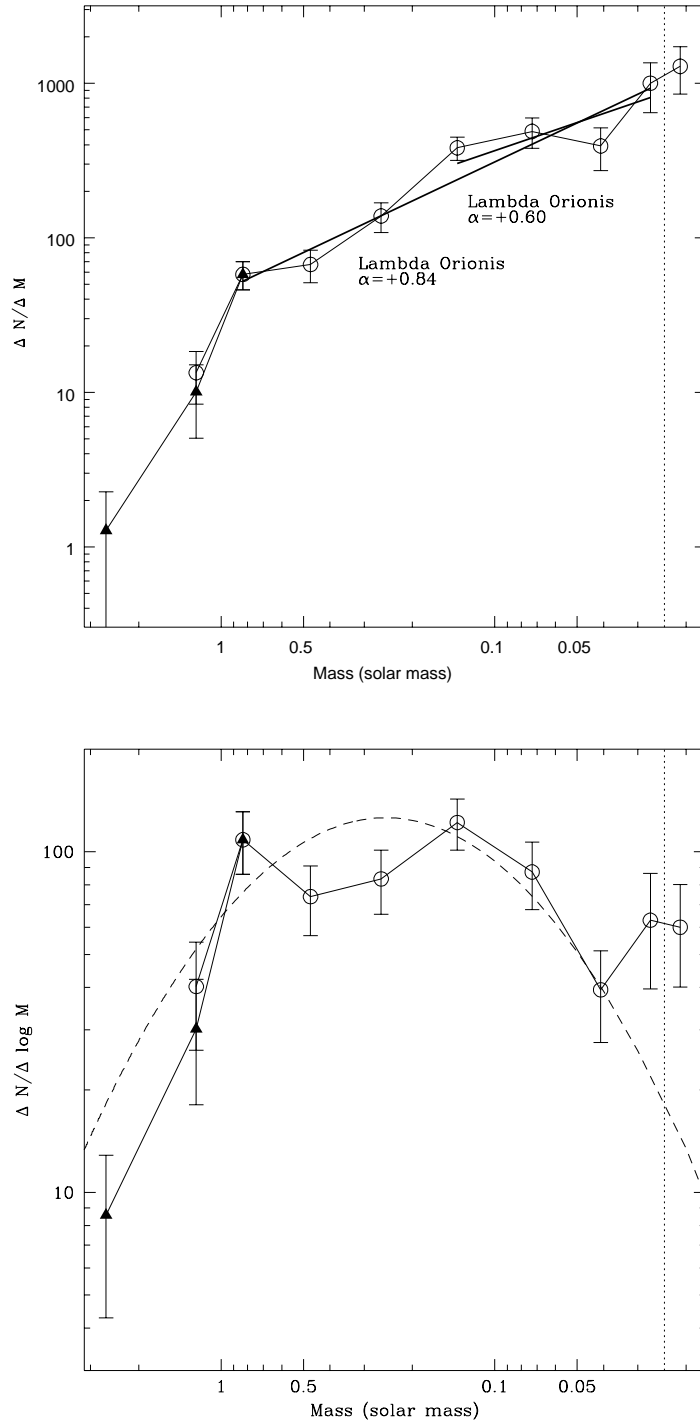


Fig. 10.— Initial Mass Function for the Lambda Orionis cluster. **a** Solid triangles and open circles correspond to data from Dolan & Mathieu (1999, 2001) and this work –same area, respectively. The vertical segment corresponds to the completeness limit. **b** Mass Function for Lambda Orionis -solid line- and the Pleiades (dashed curve, Moraux et al. 2003) in lognormal form.

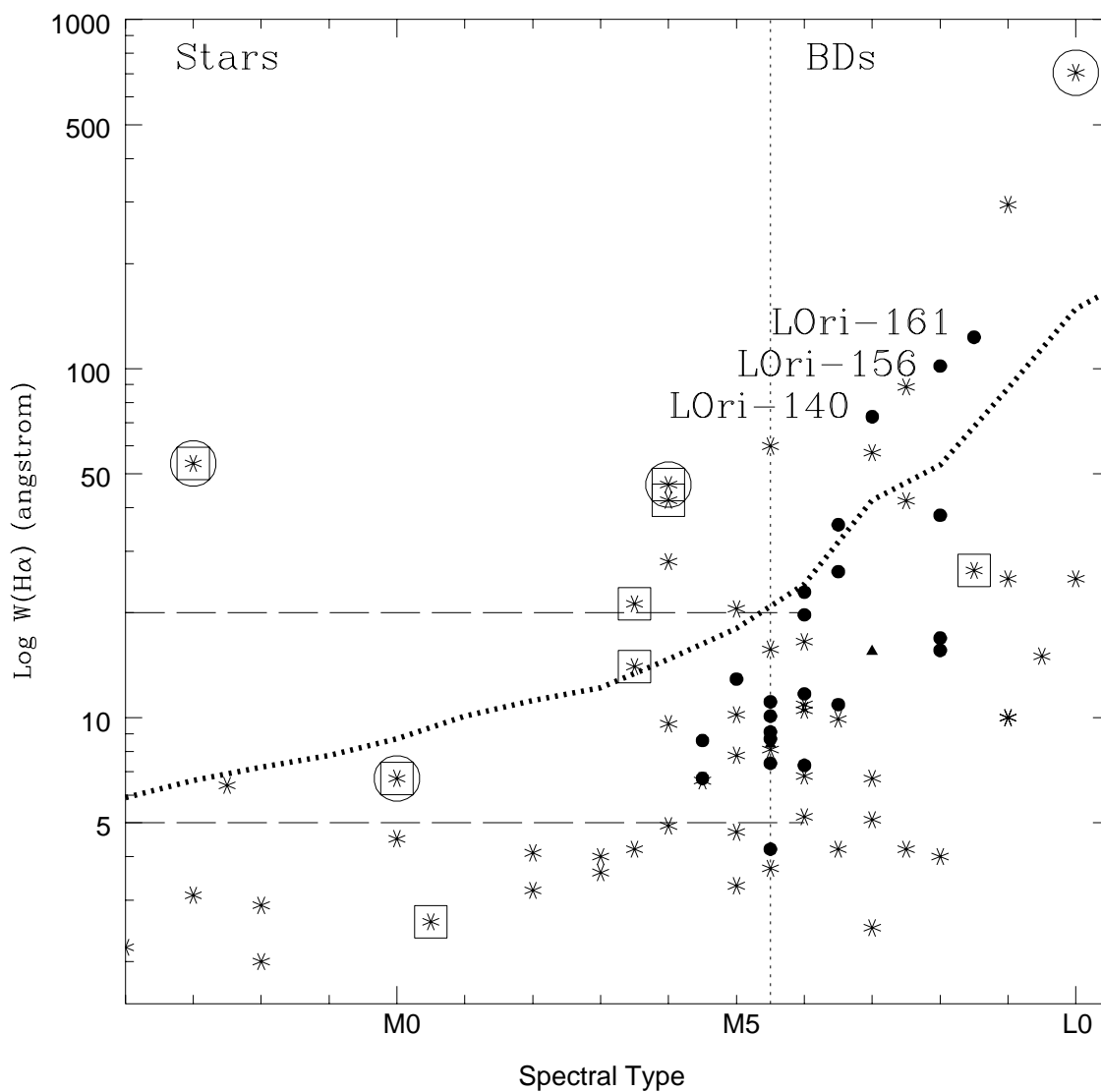


Fig. 11.— H(α) equivalent width versus the spectral type. The values for Lambda Orionis candidate members (open circles for "NM+", solid triangles for "Mem?", and solid circles for "Mem+") are compared with members of the "twin" cluster sigma Orionis (asterisks). Big circles and squares indicate sigma Orionis members having infrared excesses and forbidden lines in the spectrum, respectively. The dashed lines indicate two traditional criteria which separate Weak-line from Classical T Tauri stars (5 and 20 \AA). The light, vertical dotted line indicates the expected separation between stars and BDs at 5 Myr. The thick dotted line corresponds to the criteria differentiating accreting from non accreting objects, based on low resolution spectroscopy (Barrado y Navascués & Martín 2003).